

1 **Response to the Editor's comment**

2 **The authors thank the Editor for the additional comments provided and related to**
3 **some final inconsistencies in the text compared to the recommendations provided**
4 **by the two anonymous reviewers. All the points raised by the Editor has been fixed**
5 **in the final version. Below we provided the text adjustments in track changes.**

6 **The authors want to stress that now there is full consistency between Figure 3 and**
7 **the table in the Appendix, while a comment is provided to clarify the removal of the**
8 **repeated text at the Lines 544-553 of the manuscript version 1.**

9
10
11

12 **Use of automatic radiosonde launchers to measure temperature and humidity**
13 **profiles from the GRUAN perspective**

14

15 Fabio Madonna¹, Rigel Kivi², Jean-Charles Dupont³, Bruce Ingleby⁴, Masatomo Fujiwara⁵, Gonzague
16 Romanens⁶, Miguel Hernandez⁷, Xavier Calbet⁷, Marco Rosoldi¹, Aldo Giunta¹, Tomi Karppinen²,
17 Masami Iwabuchi⁸, Shunsuke Hoshino⁹, Christoph von Rohden¹⁰, Peter William Thorne¹¹

18

19 ¹Consiglio Nazionale delle Ricerche - Istituto di Metodologie per l'Analisi Ambientale (CNR-IMAA), Tito Scalo (Potenza), Italy

20 ²Finnish Meteorological Institute, Helsinki, Finland

21 ³Institut Pierre et Simon Laplace (IPSL), Paris, France

22 ⁴European Centre for Medium-range Weather Forecasts (ECWMF), Reading, UK

23 ⁵Hokkaido University, Sapporo, Japan

24 ⁶MeteoSwiss, Payerne, Switzerland

25 ⁷Agencia Estatal de Meteorología, Madrid, Spain

26 ⁸Japan Meteorological Agency (JMA), Tokyo, Japan.

27 ⁹Aerological Observatory, Tsukuba, Ibaraki, Japan.

28 ¹⁰Deutscher Wetterdienst (DWD), GRUAN Lead Centre, Lindenberg, Germany.

29 ¹¹Irish Climate Analysis and Research Units, Dept. of Geography, Maynooth University, Maynooth, Ireland.

30

31 **Abstract**

32 In the last two decades, technological progress has not only seen improvements to the quality of
33 atmospheric upper-air observations, but also provided the opportunity to design and implement
34 automated systems able to replace measurement procedures typically performed manually.
35 Radiosoundings, which remain one of the primary data sources for weather and climate
36 applications, are still largely performed around the world manually, although increasingly fully
37 automated upper-air observations are used, from urban areas to the remotest locations, which
38 minimise operating costs and challenges in performing radiosounding launches. This analysis
39 presents a first step to demonstrating the reliability of the Automatic Radiosonde Launchers (ARLs)
40 provided by Vaisala, Meteomodem and Meisei. The metadata and datasets collected by a few
41 existing ARLs operated by GRUAN certified or candidate sites (~~Sodankylä~~, Payerne, Trappes,
42 Potenza) have been investigated and a comparative analysis of the technical performance (i.e.

Eliminato: Sondakyla

44 manual vs ARL) is reported. The performance of ARLs is evaluated as being similar or superior to
45 those achieved with the traditional manual launches in terms of percentage of successful launches,
46 balloon burst and ascent speed. For both temperature and relative humidity, the ground check
47 comparisons showed a negative bias of a few tenths of a degree and % RH, respectively. Two
48 datasets of parallel soundings between manual and ARL-based measurements, using identical sonde
49 models, provided by Sodankylä and Faa'a stations showed mean differences between the ARL and
50 manual launches smaller than ± 0.2 K up to 10 hPa for the temperature profiles. For relative
51 humidity, differences were smaller than 1% RH for the Sodankylä dataset up to 300 hPa, while they
52 were smaller than 0.7% RH for Faa'a station. Finally, the observation-minus-background (O-B) mean
53 and rms statistics for German RS92 and RS41 stations which operate a mix of manual and ARL launch
54 protocols, calculated using the ECMWF forecast model, are very similar, although RS41 shows larger
55 rms(O-B) differences for ARL stations, in particular for temperature and wind. A discussion on the
56 potential next steps proposed by GRUAN community and other parties is provided, with the aim to
57 lay the basis for the elaboration of a strategy to fully demonstrate the value of ARLs and guarantee
58 that the provided products are traceable and suitable for the creation of GRUAN data products.

59

60 **1. Introduction**

61 Radiosondes are one of the primary sources of upper-air data for weather and climate monitoring.
62 Despite the advent and the fast integration of GNSS-RO (radio occultation) as an effective source of
63 upper-air temperature data (Ho et al., 2017), radiosondes will likely remain an indispensable source
64 of free-atmosphere observational data into the future. Radiosonde observations are applied to a
65 broad spectrum of applications, being input data for weather prediction models and global
66 reanalysis, nowcasting, pollution and radiative transfer models, monitoring data for weather and
67 climate change research, and ground reference for satellite and also for other in-situ and remote
68 sensing profiling data.

69 The analysis of historical radiosonde data archives has repeatedly highlighted that changes in
70 operational radiosondes introduce clear discontinuities in the collected time series (Thorne et al.,
71 2005; Sherwood et al., 2008; Haimberger et al., 2011). Moreover, where radiosonde observations
72 have been used in numerical weather prediction, systematic errors have sometimes been
73 disregarded and the instrumental uncertainties have been estimated in a non-rigorous way
74 (Carminati et al., 2019). Nowadays, there is a broad consensus on the need to have reference
75 measurements with quantified traceable uncertainties for scientific and user-oriented applications.
76 The GCOS Reference upper-air network (GRUAN) provides fundamental guidelines for establishing

77 and maintaining reference-quality atmospheric observations which are based on principal concepts
78 of metrology, in particular, traceability (Bodeker et al., 2016).

79 Apart from direct instrument performance aspects of the radiosounding equipment and radiosonde
80 model, it must be acknowledged that there are many challenges in performing radiosounding
81 launches. During the preparation and launch phase, many circumstances may interfere with the
82 smooth operation of radiosoundings such as undertaking launches at night, harsh meteorological
83 conditions for balloon train preparation, if any, and safe handling when using hydrogen as balloon
84 gas, and last but not least the risk of errors/mishandling by the operators. Additional expenditure
85 may be required when observations are performed in remote regions of the globe, including the
86 polar regions, deserts, or remote islands.

87 Since the start of radiosounding efforts in the early-to-mid 20th Century, the radiosounding systems
88 and the radiosondes themselves have radically changed in size, weight, and performance. For
89 example, a very important innovation was the automation of the data processing and message
90 production from about 1980. Of particular note is that thanks to new technologies, over recent
91 decades, three manufacturers have developed and deployed fully Automatic Radiosonde Launchers
92 (ARL) able to perform unmanned soundings.

93 ARL are robotic systems able to complete in an automatic fashion almost all of the operations
94 performed manually by an operator during radiosounding launch preparation and release, including
95 the implementation of ground check procedures. The advantages of ARLs are in the reduction of
96 the challenges described above as well as in the reduced running costs of a sounding station (e.g.
97 reduction in the need for trained staff and the trend of automating hydrogen production due to cost
98 reasons and to the helium international crisis) and in ameliorating problems of recruiting long-term
99 operators for remote locations. Nevertheless, it must be also stressed that the system must be
100 regularly stocked and maintained to avoid major issues and high repair costs being incurred. In
101 addition, with changes in the radiosonde technology, updates of the systems might be required to
102 enable the use of a new radiosonde type, with periodical costs (variable, every 3-6 years) which
103 might be substantial for a station. In 2018, NOAA-NCEI published stories on its website which show
104 the potential benefits of using ARLs (<http://www.noaa.gov/stories/up-up-and-away-6-benefits-of-automated-weather-balloon-launches>). Within these stories as well as from the feedback collected
105 within the GRUAN community, several radiosonde stations have reported benefits from the use of
106 ARL and an increase in the percentage of successful soundings with a potential reduction of missing
107 data in the collected data records.

109 Using recent ECMWF statistics on the number of stations transmitting data to the WMO Information
110 System (WIS) and information provided by the GRUAN community and others, there are about 90
111 ARLs (Figure 1) providing data versus about 700 manual stations. ARL stations cover many countries
112 and remote regions, including Arctic and Antarctic locations as well as a broad suite of remote Pacific
113 and other island locations. As far as is known many of the ARL stations only make automated
114 launches. In addition, there are a few more stations, used by research institutions or environmental
115 agencies, not transmitting data via the Global Telecommunication System (GTS) of the WMO
116 Information System (WIS). The total number of stations operating an ARL worldwide has increased
117 within the last decade (see Table A1 and A2 in Appendix A).

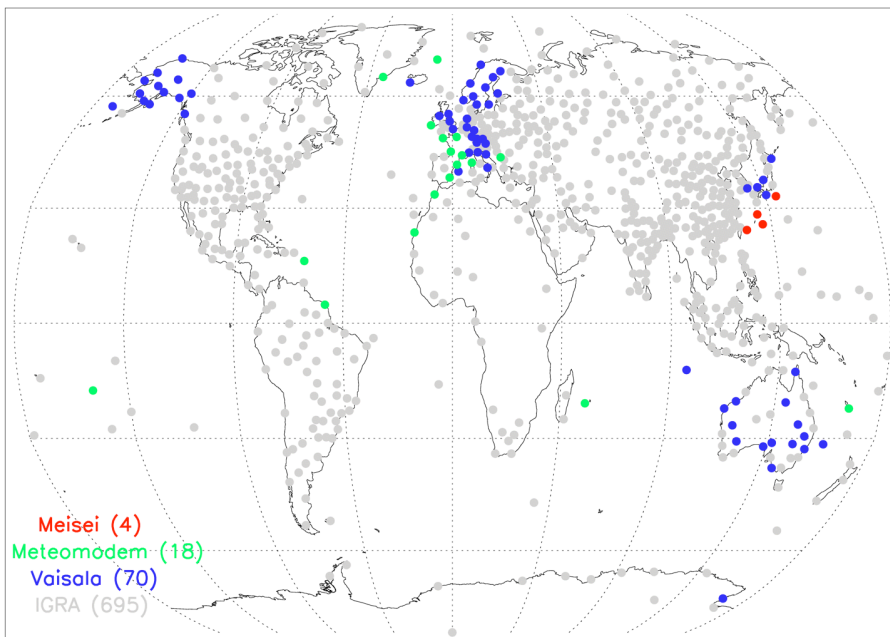
118 Vaisala introduced its first automatic system in 1990, Meisei in 2006 and Meteomodem in 2009.
119 Despite their relatively recent development and deployment, ARLs appear to be successful, and the
120 number of deployed systems will likely increase in the future. However, to date there are very few
121 peer-reviewed papers in the literature dealing with ARLs or comparing ARL vs manual data (often
122 limited to specific examples, e.g. Madonna et al., 2011). More specifically, there is currently no side-
123 by-side assessment of quality in comparison to manually launched sondes. The aim of this paper is
124 thus to quantify the reliability and stability of ARLs and assess the accuracy of their data compared
125 to the traditional manual systems. A discussion on the measurement traceability and on the
126 feasibility to use ARLs in a regular way in the GCOS Reference Upper Air Network (www.gruan.org)
127 is also provided. At present, traceability to SI standards is quantified at several GRUAN sites by the
128 use of a Standard Humidity Chamber (SHC) which can be used for ARL before the launcher loading
129 only. The SHC is a simple ventilated chamber (~4 – 5 m/s) using distilled water which, during the
130 ground check procedure, is first heated a few degrees above ambient temperature and then cooled
131 to saturate air at 100% relative humidity. The SHC allows a check of each radiosonde at 100% RH
132 using distilled water (or other RH values using solutions with specific salts although these are
133 generally only used at the GRUAN Lead Centre and for sonde characterisation and not operational
134 sounding preparation purposes).

135 The comparison reported in this paper focuses exclusively on temperature and relative humidity
136 profiles and relies upon manufacturer's products (i.e. GRUAN Data Processing based on the raw
137 data collected by the sonde, described in Dirksen et al., 2014, and Kobayashi et al., 2019, is not
138 used).

139 The remainder of the paper is structured as follows. In section 2, a short description of the three
140 ARLs is provided. In section 3, the technical performance of the ARLs is investigated on the basis of

141 statistics comparing the technical efficiency of the ARLs versus the manual sounding stations as well
142 as reporting an analysis of the feedback from station operators collected at the GRUAN sites on the
143 advantages, limitations and technical issues faced to maintain and ensure continuity of ARL
144 operations. Section 4 reports on the effect of the usage of ARLs on the stability and the accuracy of
145 ground-check calibration procedures. Section 5 provides statistics obtained from parallel soundings
146 at different sites for both temperature and humidity profiles. Section 6 discusses the comparison
147 between observation-minus-background (O-B) statistics obtained from ARL data and manually
148 launched data, respectively, using the ECMWF short-range forecast fields. Finally, section 7 provides
149 a summary and a description of the experiments which might be performed to design future ARL
150 setup to enable full measurement system traceability to SI units and, therefore, to meet GRUAN
151 requirements for long term reference climate data.

152



153

154 Figure 1: Map of stations running an Automatic Radiosonde Launcher (ARL) and transmitting the data to the WIS in late
155 2019 (see also Appendix A). Blue dots are the Vaisala ARL, green the Meteomodem, and red the Meisei. In light grey,
156 the manual stations providing data to the WIS in September are also reported. Number of stations for each color is
157 reported in brackets.

158

159 **2. Description of existing ARL systems**

160

161 **2.1 Vaisala Autosonde: brief history and recent system configurations**

162 Automation of upper-air sounding data processing has made steady progress since the early 1970's
163 and is now widespread (Kostamo, P., 1992). The Vaisala Autosonde project was started in late 1992
164 and a working prototype presented at CIMO, Vienna, in 1993. The prototype was tested in Norway
165 and Sweden in 1993 and 1994. This coincided with the replacement of manual balloon tracking
166 systems by Omega and Loran networks. It was provided by Vaisala Oy (Finland) and was
167 permanently installed at the Landvetter station in Sweden in 1994. As of today, about 80 Vaisala
168 ARLs have been installed worldwide and the number of soundings performed has exceeded
169 800,000, while the annual number of new soundings will soon exceed 70,000 (Lilja et al., 2018).
170 With the newest Autosonde model it is possible to perform 60 soundings without replenishment,
171 while the earlier models allowed up to 24 soundings.

172 The first radiosonde type used for an automatic launch was the RS80-15N (during 1994-2006). The
173 RS80 radiosonde was followed by the models RS92 (manufactured 2005-2017) and then RS41
174 (available since late 2013). The RS92 radiosonde (Dirksen et al. 2014) performs measurements with
175 a nominal measurement uncertainty (provided by the manufacturer) of 0.5°C for temperature, 1.0
176 hPa for pressure below 100 hPa and 0.6 hPa above, 0.15 m s⁻¹ for wind speed and 5 % RH for relative
177 humidity ([https://www.vaisala.com/sites/default/files/documents/RS92SGP-Datasheet-](https://www.vaisala.com/sites/default/files/documents/RS92SGP-Datasheet-B210358EN-F-LOW.pdf)
178 [B210358EN-F-LOW.pdf](https://www.vaisala.com/sites/default/files/documents/RS92SGP-Datasheet-B210358EN-F-LOW.pdf)). RS41 sonde specifications for nominal measurement uncertainties
179 (provided by the manufacturer) are 0.3°C for temperatures below 16 km and 0.4°C above, 0.01 hPa
180 for pressure sensor, 0.15 m s⁻¹ for wind speed and 4 % RH for relative humidity
181 (<https://www.vaisala.com/sites/default/files/documents/RS41-SGP-Datasheet-B211444EN.pdf>).

182 Note that the Vaisala RS41 radiosondes are of two different types: RS41-SG which are not equipped
183 with a pressure sensor and using the GNSS-based method to infer pressure (Lehtinen, 2014), and
184 RS41-SGP which uses a pressure sensor as the default. More stations use the RS41-SGP than the
185 RS41-SG: in November 2019, 158 stations type were using RS41-SGP versus 66 stations using type
186 RS41-SG.

187 To launch the RS41 sondes, the Autosonde Ground Check (GC) procedure has been updated. The
188 GC device of the RS41 sondes consists of a wall-mounted box and an activator that contains a
189 wireless reader for the radiosonde. The device is designed to automatically activate the radiosonde
190 and to enable wireless data transfer. An activator is connected to the reader box with a coaxial

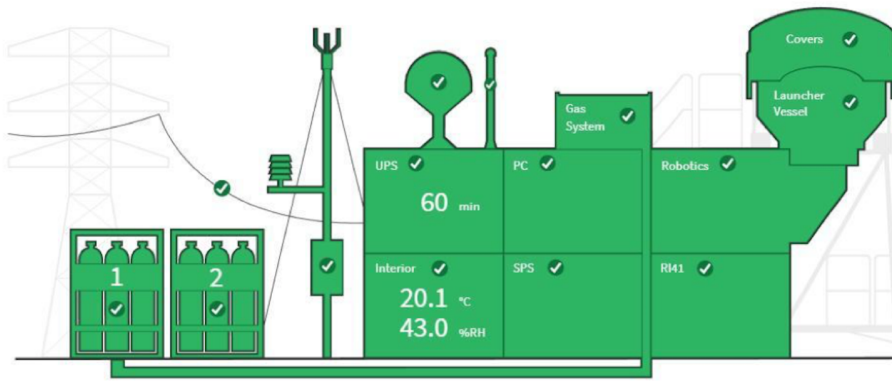
191 cable. The ground check device also includes a barometer while the surface pressure used as a
192 reference for the launch is obtained from a separate co-located automatic weather station.
193 However, the ground check pressure device can be used as a backup for the weather station sensor.
194 The GC performs a temperature check where the actual temperature sensor is compared with the
195 one integrated on the humidity sensor chip. In contrast to the RS92 GC, a pre-flight fine-tuning of
196 the temperature measurement is no longer applied to the RS41 because the manufacturer found
197 that the performance of the RS41 temperature measurement is practically unchanged during
198 storage.

199 Humidity is also checked in the GC. The RS41 humidity check consists of two main steps – the sensor
200 reconditioning phase and the 0% RH check. In the reconditioning phase, the sensor is heated to
201 remove possible contaminants that might affect the measurement results and cause a slight
202 degradation of the sensitivity of the humidity sensor. Then, the humidity sensor is checked and then
203 corrected against a dry humidity condition. Specifically, the dry reference condition of the new zero
204 humidity check is generated in open air by heating the sensor using the integrated heating element
205 on the sensor chip. The procedure is based on the decrease of relative humidity towards zero as the
206 temperature rises high enough (Vaisala, 2013; Vaisala 2015). This method differs from the RS92 GC
207 where the correction was based on a dry condition generated with desiccants, whose drying
208 capacity gradually fades with time.

209 The radiosonde's humidity sensor is reconditioned and ground check performed during the
210 automated launch preparation in order to ensure similar performance as in manual stations (Lilja et
211 al., 2018). The top panel of Figure 2 provides a schematic picture of the most recent VAISALA AS41
212 Autosonde system configuration while the bottom panel shows a photograph of the Autosonde
213 system operational at the Finnish Meteorological Institute GRUAN site in Sodankylä (WIGOS station
214 identifier=0-20000-0-02836, 67.34 °N, 26.63 °E, 179 m a.s.l.). In Table 1, the basic technical data of
215 the Autosonde AS41 are reported. More details on the specifications of the Vaisala Autosonde AS41
216 can be found in the datasheet (B211636EN-A_2 pages.pdf, last accessed September 20, 2019)
217 available on the Vaisala website (<https://www.vaisala.com>).

218

219



220
221
222
223
224
225
226
227
228
229
230

Figure 2: Schematics of the VAISALA Autosonde AS41 system in its most recent configuration (top panel), and photo of the Autosonde system AS15 (bottom panel) operational at the Finnish Meteorological Institute GRUAN site in Sodankylä (WIGOS station identifier=0-20000-0-02836, 67.34 °N, 26.63 °E, 179 m a.s.l., see Vaisala 2018, https://www.vaisala.com/sites/default/files/documents/AUTOSONDE%20AS41%20Datasheet%20B211636EN-A_2%20pages.pdf).

231 Table 1: Autosonde AS41 technical data (Vaisala, 2018)

Dimensions	Width: 3.30 m
	Length: 7.80 m
Launch Tube Diameter	2.20 m
Height during transport	2.90 m
Total height with launcher tube	5.10 m
Gross weight with launcher tube	7.5 t
Electrical energy consumption	< 1 kW (without air conditioning)

232
233

234 2.2 Meteomodem Robotsonde

235 The Meteomodem ARL is an automatic balloon launcher system that can perform up to 12 or 24
236 soundings without any manual control (<http://www.Meteomodem.com/docs/en/Leaflet-robotsonde.pdf>). The system is compatible with M10 and M20 Meteomodem radiosonde types. It
237 is built in a robust dry maritime container and composed of the following subsystems (Figure 3):
238

- 239 • Operator room with electronic control unit and PC workstation, isolated from the launch tube
240 by an air-tight safety door, and used only during radiosonde setup and restocking;
- 241 • Carrousel with 12 or 24 removable containers for balloon trains, and with individual flexible
242 cover on balloon locations which preserve balloons from desiccation;
- 243 • Launch tube for balloon inflation and release and pneumatic equipment or pressurized air
244 network;
- 245 • Optionally, a double-door entrance to protect from strong winds, rain, drifting snow or
246 sandstorms.

247 The Meteomodem ARL main specifications are reported in Table 2. Worldwide there are 19
248 Meteomodem ARL systems automatically launching Meteomodem M10 radiosondes. The
249 specifications for nominal measurement uncertainties (provided by the manufacturer) are 0.58°C
250 for temperature, 1 hPa for pressure, 0.15 m s⁻¹ for wind speed and 5 % RH for relative humidity
251 (www.Meteomodem.com/docs/en/Leaflet-m10.pdf).

252

253

Table 2: Meteomodem ARL specifications

Dimensions	Width: 2.44 m
	Length: 6.00 m
Launch Tube Diameter	2.00 m
Height during transport	3.10 m
Total height with launcher tube	3.60 m
Gross weight with launcher tube	3.5 t
Electrical energy consumption	< 1 kW (without air conditioning)

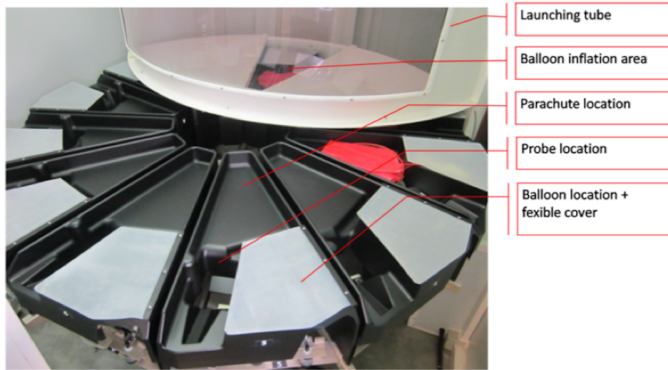
254

255

256 For each launch, there is a preparation phase which comprises the radiosonde GC and the loading
257 of the balloon train (with the radiosonde, the unwinder, the parachute, and the balloon) into
258 individual bins before finally sounding parameters (e.g. launch time schedule, inflation volume, etc.)
259 are setup.

260 During the launch phase, before powering on the sonde, the system performs a scan of the
261 bandwidth in order to detect possible radio interference, then the radiosonde battery pack is
262 powered on through an infrared link. According to the scan result, the system sets up the new
263 frequency through an infrared link, and GNSS signal collection is initialized. Then, the system loads
264 the calibration data of the relevant radiosonde stored during the preparation phase and checks
265 consistency with PTU criteria. The Meteomodem ARL GC is a standard Meteomodem GC which
266 consists of a sealed box enclosing a reference and a fan which homogenises the inside temperature
267 and relative humidity. It is recommended to return the Meteomodem GC every 3 years for
268 calibration. The calibration is made with a certified Rotronic HC2A-S probe
269 (<https://www.rotronic.com/en/hc2a-s.html>).

270 Then, the ARL records the ground check data and the metadata. Balloon inflation starts accordingly:
271 the system monitors a flowmeter to inflate the balloon to the specified volume. The ARL may use
272 either helium or hydrogen gas. Finally, the balloon is released at the specified launch time. In case
273 of launch failure before balloon release or during the flight, the procedure will restart for a new
274 sounding immediately or can alternatively be manually launched according to a preset time
275 schedule. At any time, an immediate start of the launch procedure can be initiated by an operator
276 (locally or remotely).



279
280
281
282
283
284

Figure 3: Meteomodem Robotsonde (top panel) launching a balloon at Trappes station (WIGOS station identifier=0-20000-0-07145, 48.77N, 2.01E, 168 m asl, <http://www.Meteomodem.com/robotsonde.html>) and photograph of the carousel of Meteomodem Robotsonde with the balloon location (bottom panel).

285 For those stations operating an ARL and adopting a protocol based on GRUAN recommendations
286 (Dirksen et al., 2014), as at Trappes station (WIGOS station identifier=0-20000-0-07145, 48.77N,
287 2.02E, 168 m asl, top panel of Figure 2.2), the GRUAN M10 ground check procedure is performed in
288 two steps: 5 minutes in a ventilated hut in ambient conditions together with calibrated T and RH
289 sensors and, further, another 5 minutes to test the radiosonde performance in the SHC. Then each
290 radiosonde is loaded in the ARL carousel (bottom panel of Figure 3).

Eliminato: 46
Eliminato: 0
Eliminato: .20

294 A technical document describing the M10 sensor, corrections and uncertainties for both the
295 temperature and relative humidity sensors will become available through the GRUAN community
296 as soon as a Meteomodem M10 GRUAN data product is available.

297

298 **2.3 Meisei Automated Radiosonde System**

299 The Meisei ARL, named “Automated Radiosonde System” is designed for fail-safe operation and
300 high remote operability. Compared to the previous version developed in 2006, the new system, still
301 under improvement, is able to load more radiosondes thanks to the development of the Meisei
302 “Canister Type”. The operator can preload a maximum number of 40 sondes in the so-called
303 "Canister modules". The canister has been recently implemented to reduce failures. Once the
304 launch procedure has started, the respective canister fills a balloon independently. The right
305 canister module and the left canister module are independent systems. It realizes high observation
306 continuity by duplicating gas, air and electric systems. The canister module on one side can be
307 moved to the preparation room to load the sonde and facilitate the operator’s work. The new ARL
308 version can also recover from balloon bursts without human intervention at the site by using a
309 balloon from another canister. In the previous version, an operator had to visit the ARL to remove
310 broken balloons and restart the ARL during the observation window in such cases.

311 The new system is also equipped with a new simplified wind shield for launches in strong wind
312 conditions. All information and data are stored in a database available for each ARL. Various central
313 monitoring/control functions are provided by using application software and a web browser to
314 access the database on the workstation installed in the ARL. The Meisei ARL GC consists of a
315 temperature and humidity reference sensor and an inspection box. The GC is performed before the
316 sonde loading. The results from the GC are not used in the data processing but only to check if there
317 are anomalies in the radiosondes.

318 In Table 3, the Meisei Automated Radiosonde System specifications are provided. Figure 4 shows a
319 photo of the system along with a sketch of the internals of system container. For more details on
320 the Meisei ARL experimental setup visit the Meisei website (<http://www.meisei.jp/ars>). Japan
321 Meteorological Agency (JMA) has used Meisei ARLs data since 2006. Parallel radiosoundings of auto
322 launch and manual launch have not been done yet. This is the reason why this paper does not show
323 additional datasets or comparisons involving Meisei ARL; therefore, the description of the Meisei
324 ARL is the only information which can be shared with readers, according to recommendations
325 provided by Meisei.

326

327

Table 3: Meisei ARS specifications

Dimensions	Width: 2.50 m
	Length: 6.20 m
Launch Tube Diameter	2.20 m x 1.80 m square
Height during transport	3.10 m
Total height with launcher tube	1.90 m (2.80 m including windshield)
Gross weight with launcher tube	6 t
Electrical energy consumption	< 1 kW (without air conditioning)

328

329

330 3. Technical performance

331

332 Beyond the automation of the radiosonde launch procedure, there are two main differences

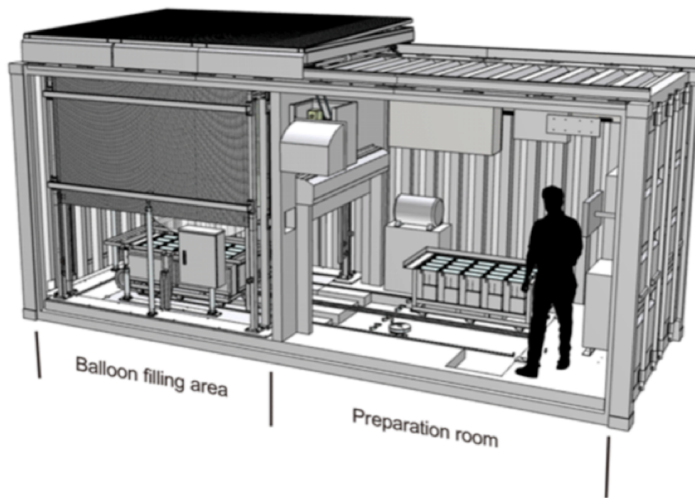
333 between an ARL and a manual launch:

334 ● Ground check procedures may be performed only during the sonde loading in the carousel
335 chamber, days or weeks before the sonde launch, though there is a trend towards less
336 frequent stocking;

337 ● The use of independent and traceable calibration standards like the Standard Humidity
338 Chamber (SHC) is possible but only before the launcher loading (also in this case one or more
339 days before the launch).

340 Both these aspects will be discussed in the following sections which provide potential technical
341 solutions to address the gaps between manual and automatic launch procedures in terms of
342 performance and traceability.

343



344

345 Figure 4: Picture of a Meisei Automatic Balloon Launcher (top panel) and sketch of the internals of ARL container in its
346 most updated configuration (bottom panel).

347

348 This section aims to provide a classification of the main challenges met by the stations which have
349 operated ARLs over several years and to assess the technical performance of the ARLs compared to
350 manual launches. The section is built upon the feedback provided by the GRUAN sites in response
351 to a survey for the collection of ARL information. Most of the ARLs at GRUAN sites are from Vaisala
352 (thus the analysis is not representative of Meisei and Meteomodem systems due to the very limited
353 feedback available for these systems). Given the small sample size, this is presented qualitatively

354 rather than quantitatively and it is anonymised. Examples of technical performance in the field are
355 then provided for a Vaisala and a Meteomodem ARL operating the most recent updated version of
356 the respective manufactured systems (at Payerne and Trappes stations).

357 A conceptual diagram to represent a generic ARL is provided in Figure 5: each ARL can be
358 schematically divided into 4 areas as follows:

- 359 ● the operator's area, where the operators can manage the system, prepare radiosondes and
360 balloons to be uploaded and where the station reception and processing units are located;
- 361 ● the ready-to-launch sondes storage area, built around the ARL rotating trays, where most
362 of the automated technologies are implemented to allow a completely unmanned launch;
- 363 ● the launching vessel area, where the balloon is filled and becomes ready for the launch;
- 364 ● external area, where all the ancillary instruments, such as the weather station and GNSS
365 antenna, are located along with gas tanks.

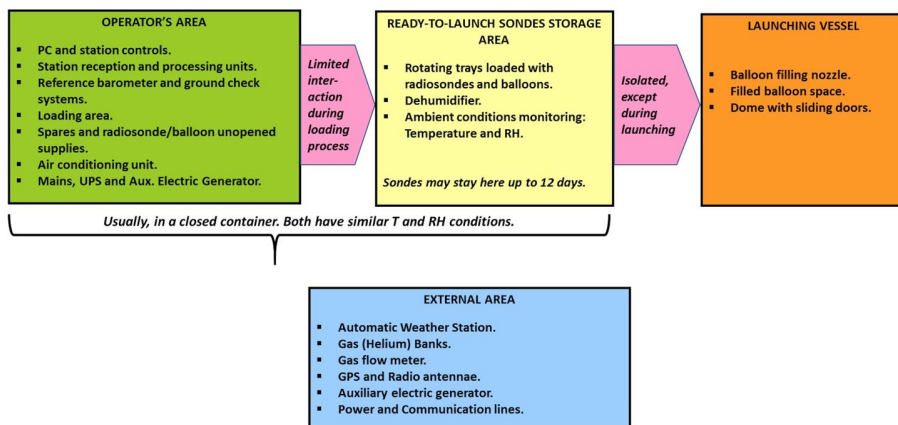
366 For each area, the weakest points identified from the GRUAN sites operating an ARL are:

- 367 ● in the operator's area, most of the issues are related to the not infrequent failure of power
368 supply system or of the air conditioning system, often related to a major failure of the power
369 supply at the measurement station itself. This represents a particular weakness in the use
370 of ARLs in remote areas where power supply is generally less stable, and where logically the
371 ARL might be an obvious choice. A few sites also reported issues in the software and logic
372 controllers;
- 373 ● the ready-to-launch sonde storage area is assessed as the most efficient part of ARLs, where
374 few issues reported. The most critical issue identified in this area is the infrequent failure of
375 the air compressor;
- 376 ● the launching vessel area is where the balloon is filled and launched and where, therefore,
377 we have a high exposure to many environmental factors like harsh climate, dust, animals,
378 etc., which can strongly affect a successful launch also with later effects to the balloon and
379 early burst. Several issues were raised by the stations related to challenges in the balloon
380 inflation process, failure of balloon presence sensor allowing launch of under-inflated
381 balloons, gas tubes bent and frozen gas hoses, balloon blocked on the tray, failure of the
382 rams which open vessel cover doors (this concerns Vaisala or Meisei, and not Meteomodem
383 ARL). Other issues noted were delays in launch detection time compared to the actual
384 launch time, and occasional break of the radiosonde string at launch (for Meisei);

385 ● the external area, is another critical area where several problems have been reported about
 386 the gas flow meter and the switching between the gas tanks (one close to empty and the
 387 other fully filled). Extreme weather conditions (e.g. very strong winds) can make the launch
 388 more difficult, despite the additional screens protecting the balloon flight in the first 2-3
 389 meters above the ARL (only for Vaisala and Meisei).

390 The problems listed above are not common to all the ARLs, each system has its own specific issues.
 391 While the feedback reported from GRUAN stations can provide a first assessment of the challenges
 392 in operating an ARL, this study cannot assess challenges in the operation of each specific model and
 393 it cannot quantify the improvements of each ARL with the time. The issues discussed above could
 394 be used as recommendations to the manufacturers to foster further improvements of the systems.
 395 The ARLs are typically maintained by the manufacturers on an annual check up (performed
 396 remotely) and major maintenance approximately every 3 years. This maintenance schedule, if
 397 applied at each station can increase the reliability of the systems over both the short- and long-
 398 term, although it generates additional costs.

399



400

401

402 Figure 5: Conceptual diagram of a typical automatic radiosonde launcher divided in four main areas: operator's area
 403 (green), ready-to-launch sondes storage area (yellow), launching vessel area (orange) and external area (cyan).

404

405 To assess the effective technical performances of the ARL launches vs manual launches, in Table 4
 406 and 5, examples of the statistics collected at two GRUAN sites running an ARL, Payerne (WIGOS
 407 station identifier=0-20000-0-06610, 46.82N, 6.93E, 490m asl), operated by MeteoSwiss, and
 408 Trappes, operated by Meteo France, respectively, are reported. The Table provides a summary of

409 pertinent characteristics of the ARL versus manual launches. For Payerne, statistics are related only
410 to the automatic and manual launches performed since April 2018 (on average, ARL nine per week,
411 manual five per week) using the Vaisala AS15 ARL. For Trappes, manual launches were performed
412 in the period 2012-2014, while the Meteomodem Robotsonde has been operated in the period
413 2016-2018; in both cases two launches per day were performed with similar daily scheduling.
414 At Payerne, since April 2018 the Vaisala ARL has realized 470 successful flights per year, according
415 to MeteoSwiss standards¹, while manual launches have been 260 per year. Despite the use of
416 different balloon sizes due to the fact that for manual launches bigger balloons are often used to
417 perform ozonesoundings, the percentage of successful launches as well the percentage of sondes
418 reaching 10 hPa pressure level is indistinguishable between the ARL and the manual launches, with
419 a limited use of spare sondes due to the failure of scheduled launches for the ARL (4 %). Ascent
420 speed statistics are very close with better performance of the ARL in preventing very low balloon
421 gas filling and thus slow ascents.

422 At Trappes station (Table 5), during the period January 2016 to December 2018, the Meteomodem
423 ARL Robotsonde has carried out 1908 successful flights, according to MeteoFrance standards², out
424 of a total of 1956. For each of the remaining 48 flights, a spare automatic launch was performed
425 which fulfilled the requirements of MeteoFrance. The mean percentage of successful launches is
426 97.9% (2016: 95.5%, 2017: 98.2%, 2018: 99.1%, 2019(Jan-Oct): 98.6%, see Figure 6) with an evident
427 improvement using ARL in the percentage of sondes reaching 10 hPa pressure level (80%) compared
428 to the manual launches (60 %). The use of Totex balloons is one of the reasons for the improvement
429 and further improvement was achieved by increasing the size of the balloon. Moreover, since
430 November 2016 Meteomodem has installed a flexible cover which assures that during the storage
431 the balloon is less exposed to contact with the air-conditioned environment. This seems to reduce
432 the effects of drier air on the balloon and improve its performance in terms of burst altitude
433 (standard deviation of burst altitude is reduced after the installation of the cover – not shown). For
434 the balloon ascent speed, comparison statistics between ARL and manual launches show also similar
435 results. According to the information shared by Meteomodem, it is also possible to add that,
436 compared to all the ARLs operated at other sites during the same period reported in Table 5, the

Eliminato: realized

¹ According to MeteoSwiss, a “successful flight” is a launch with a balloon burst at a pressure lower than 100 hPa, with no telemetry lost or sensor failure.

² According to MeteoFrance, a “successful flight” is a launch with a balloon burst at a pressure lower than 150 hPa, with no telemetry lost or sensor failure.

438 Trappes ARL has typically similar failure statistics. The time evolution of the failure (Figure 6) shows
 439 that the number of spares and the number of failures by type halved in three years to reach less
 440 than 2% relative to the number of successful flights. For the 716 flights performed during 2018, the
 441 absolute number of failures is 2 for the ARL (which was a radio loss and an inflation problem), 1
 442 failure due to sensor break, no failure from the software, 1 failure which is not classified by their
 443 automated failure identification and 1 failure due to the use of ARL which can be an operator stop
 444 or an obstructed inflation tube.

445
 446 Table 4: Technical performance of automatic vs manual launches performed at Payerne station
 447 during 2018 for a Vaisala AS15 ARL. Metadata related to the sonde and balloon types are shown
 448 alongside the percentage of success for the launches performed during the reported period, the
 449 percentage of spare sondes used, the balloons bursting before reaching 10 hPa, and the maximum,
 450 minimum and average ascent speed.
 451

Station	Automatic	Manual
Station type	AS15	MW41
RS type	RS41	RS41 (+ ECC ozonesonde)
Balloon type	Totex	Totex
Balloon size	800g	800g/1200g/2000g/3000g
Number of launches	470/year	260/year
Percentage of successful flights ³	>99%	>99%
Percentage of spare	4%(spare if P>100hPa)	N/A
Sondes above 10 hPa	92% (based on 2018)	92% (based on 2018)
Max. Ascent speed	6.1 m/s	6 m/s
Min. Ascent speed	3.5 m/s	3 m/s
Avg. Ascent speed	5.2m/s	5m/s

³ Percentage of successful flights out of successful launches.

452
453
454
455

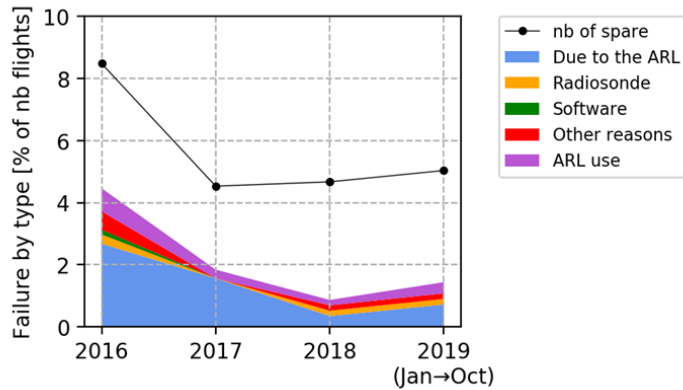
Table 5: Same as Table 4 for Trappes site in the period 2016-2018 and 2012-2014, respectively for a Meteomodem ARL.

Station	Automatic	Manual
Station type	Robotsonde (14/04/2015 to 12/2018)	SR10 (01/01/2012 to 14/04/2015)
RStype	M10	M10
Balloon type	Totex	Hwoyee
Balloon size	350g/1000g	Hwoyee 600g
Number of launches	2106	2113
Percentage of successful flights	99% (based on 2018)	>99% (based on 2012)
Percentage of spare	5% (based on 2018)	N/A
Sondes above 10 hPa	80%	60%
Max. Ascent speed	6 m/s	6 m/s
Min. Ascent speed	4 m/s	4 m/s
Avg. Ascent speed	5 m/s	5.4 m/s

456
457

458 It is worthwhile to add that ECMWF noted in some reports that some stations using Meteomodem
459 Robotsondes had anomalously dry, and sometimes warm, values just above the surface relative to
460 the background field. In cool, moist atmospheric conditions the anomalies can be two or three
461 degrees for temperature and larger for dew point temperature. "For technical reasons the launcher
462 has to be kept warm and dry internally, which means that the humidity sensor is initially reading
463 quite low and a bubble of warm/dry air escapes with the balloon at launch - the net effect is that
464 the first few decametres the dewpoint reading is too low." (Ray McGrath, pers. comm. 2015). The
465 issue described above does not affect the profile at higher levels. A similar issue has also been
466 reported for data taken during the first few seconds with Meisei ARL and this is suspected to be due
467 again to the influence of the air inside the launcher.

468 The Meteomodem has recently implemented a new software, EOSCAN, not yet implemented at all
 469 the stations, which improves the ARL dataset quality with a number of corrections such as:
 470 1. Eliminating the GPS disturbances at the end of the tube that can persist in the first 20 seconds
 471 after the release;
 472 2. Adjusting for the systematic bias introduced by the fact that the ARL Meteomodem is air
 473 conditioned and affecting the first 150 m of the radiosounding profiles.
 474



475
 476 Figure 6: Cause of failure for the Meteomodem ARL in Trappes as a function of time since the
 477 installation date. The black dots are the values of the number (nb) of spare used after the launch
 478 failure.

479

480 4. Stability, ground calibration

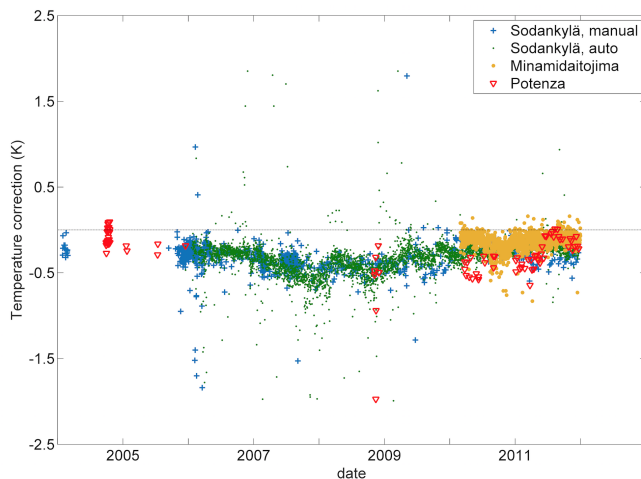
481 4.1. Performance of the Vaisala ARL

482 The performance of the Vaisala ARL has been evaluated through the analysis of a dataset collected
 483 at Sodankylä station. The Sodankylä Vaisala ARL was used to regularly launch RS92 radiosondes at
 484 11:30 and 23:30 UTC over 2006 to 2012. Manual soundings were periodically performed in parallel
 485 using a similar Vaisala DigiCora-3 sounding system throughout this period. Parallel soundings have
 486 been selected with launch time difference between 2 minutes and 20 minutes. A total of 283 parallel
 487 soundings has been considered: these are distributed evenly across the period, with the exception
 488 of 2006, which has more parallel soundings than other years, and most of these are daytime
 489 comparisons. In addition, two Vaisala ARL datasets from the Potenza GRUAN station (40.60N,
 490 15.72E, 760 m a.s.l.) and the Minamidaitojima station, run by JMA (WIGOS station identifier
 491 index=0-20000-0-47945, 25.79N, 131.22E, 15 m a.s.l.), covering a similar time period, though much

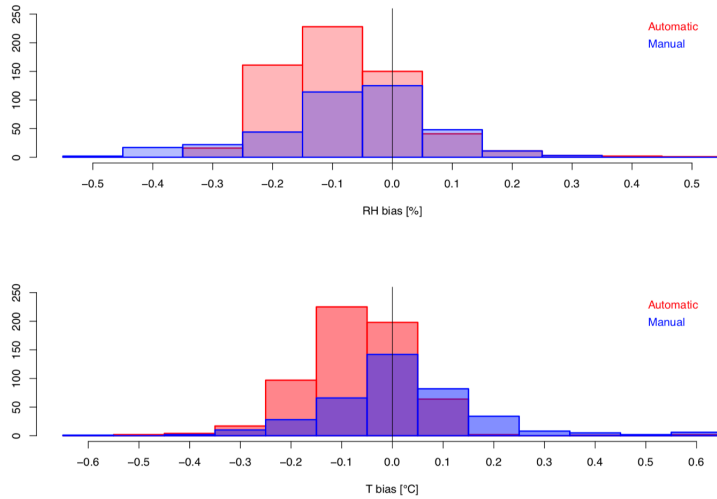
492 smaller sample sizes than in Sodankylä, have been used for comparison. Despite the less intensive
493 sampling, Potenza and Minamidaitojima data are useful data sources to compare with Sodankylä
494 and, specifically, to check consistency of the GC correction across different stations and different
495 batches of Vaisala sondes.

496 The availability of long time series of parallel sounding for the Sodankylä station permits
497 investigation of the system performance also in the pre-launch phase. Two main aspects are
498 evaluated: stability of the ground check correction on temperature, and potential effects related to
499 the time periods the sondes were stored before launch.

500 Figure 7 summarises the temperature correction applied during the GC procedure for the RS92
501 sondes of the above described data sets using the Vaisala GC25 ground check device, with most of
502 the launches performed since 2006. Figure 7 shows similar GC values at Sodankylä, Potenza and
503 Minamidaitojima stations despite the very different locations and launch scheduling, with a
504 negative adjustment of between smaller than -0.5 K before 2010 and smaller than -0.3 K typically
505 applied to most of the RS92 sondes with an improvement of the differences over the time in the
506 batches launched after 2009. The results shown in Figure 7 are based on the assumption that all the
507 reported ARL GC temperature sensors were maintained according to recommendations described
508 in the previous section.



509
510 Figure 7: Time series of the temperature correction (temperature measured by the GC reference sensor minus
511 temperature measured by the sonde) applied during the GC procedure for the RS92 sondes launched at Sodankylä, both
512 manually (blue crosses) and automatically (green dots), and at Minamidaitojima (yellow dots) and Potenza (red
513 triangles, automatically) from 2004 to 2012.



515

516 Figure 8: Distribution of temperature and relative humidity corrections found during Vaisala GC process for the
 517 automatic and the manual soundings operated at Payerne station using the RS41 radiosonde.

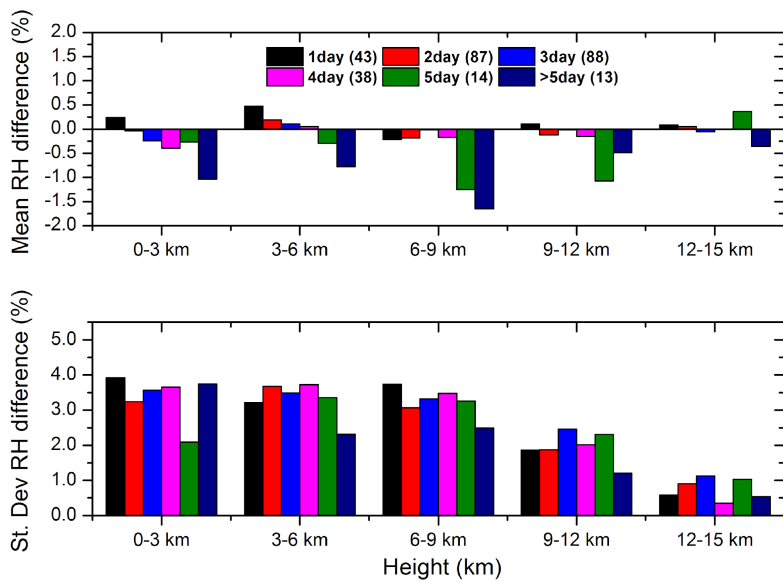
518

519 Results similar to those from Sodankylä and Potenza GRUAN stations are reported by Payerne
 520 GRUAN station (Figure 8) using the RS41 since April 2018 and operating the Vaisala AS15 ARL. Figure
 521 8 shows that the distribution of temperature and relative humidity corrections have negative
 522 skewness with the GC adjustments within a few tenths of a degree and the average adjustment is
 523 smaller than 0.1 K and 0.1% RH, respectively. These results show an average negative GC corrections
 524 for the ARL in analogy to the results reported above for RS92 sondes at Sodankylä and Potenza,
 525 where also the old Vaisala ARL version was operated. Comparisons with the broader statistics
 526 collected by GRUAN stations launching manually (not shown) reveal results consistent with the GC
 527 time series shown in Figure 7 and 8, thus excluding the presence of clear systematic effects in the
 528 GC corrections due to the use of ARLs. Nevertheless, the small differences observed between the
 529 ARL and manual GC corrections warrant further investigations to understand if performing the GC
 530 in a controlled temperature and humidity environment may generally improve or worsen the
 531 calibration in the long term.

532 In an operational station like Sodankylä, the time between balloon loading and ground check can
 533 vary from day to day. At Sodankylä average loading time was 2-3 days prior to launch for regular
 534 soundings. The ARL software allows also longer times in the tray. Figure 9 shows, at different

535 altitude ranges, the mean differences of simultaneous RH profiles (left panel) measured using the
536 ARL and the manual soundings as a function of the number of days a sonde stays on a tray before
537 launch, from 1 to more than 5 days. The corresponding mean standard deviations are also shown
538 (right panel), while in brackets within the color legend, the number of parallel soundings for each
539 time period is reported. To calculate the statistics shown in section 4 and 5, radiosounding
540 temperature and RH from parallel soundings have been interpolated to a 100-meter vertical grid.
541 Figure 9 shows that there are no RH systematic differences when parallel launches are grouped
542 according to the tray time, except for the launches with a tray time of 5 days or more at altitude
543 levels above 6 km a.g.l., where a mean difference smaller than -2.0 % RH is obtained up to 10-12 km
544 a.g.l. Nevertheless, it must be noted that the size of the sample investigated for these tray time
545 options (5 days and >5 days) is much smaller than for other tray times and these launches include
546 also parallel sounding with longer differences in the respective balloon release time.

547 To test if the estimated RH differences are meaningful, the Wilcoxon Rank Sum Test has been
548 applied. This test is a non-parametric test of the null hypothesis that it is equally likely that a
549 randomly selected value from one population will be less than or greater than a randomly selected
550 value from a second population. If the null hypothesis is rejected, then there is evidence that the
551 medians of the two populations differ. In this study, the Wilcoxon Rank Sum Test has been used
552 instead of the Z-test because of its robustness in case of a small observations sample (i.e. small
553 number of parallel launches) and to avoid assumptions on the underlying data distribution (e.g. data
554 distribution skewed or non-normal). For the RH profiles reported in Figure 9, the probability
555 computed using the Wilcoxon Rank Sum Test ranges within 0.4-0.5 with smaller values only above
556 12 km a.g.l, where the probability becomes greater than 0.2. For the time-in tray classes with a
557 smaller sample of parallel soundings (1 day, 5 day and >5 days), the probability oscillates between
558 0.05 and 0.10. Therefore, it is possible to conclude that we cannot reject the hypothesis that the
559 two data distributions (ARL and manual launches) have the same median value and the reported
560 comparisons are consistent. Finally, the bottom panel of Figure 9 shows that the standard deviations
561 are substantially smaller than 5% RH at all altitude levels without any evident correlation with tray
562 time.



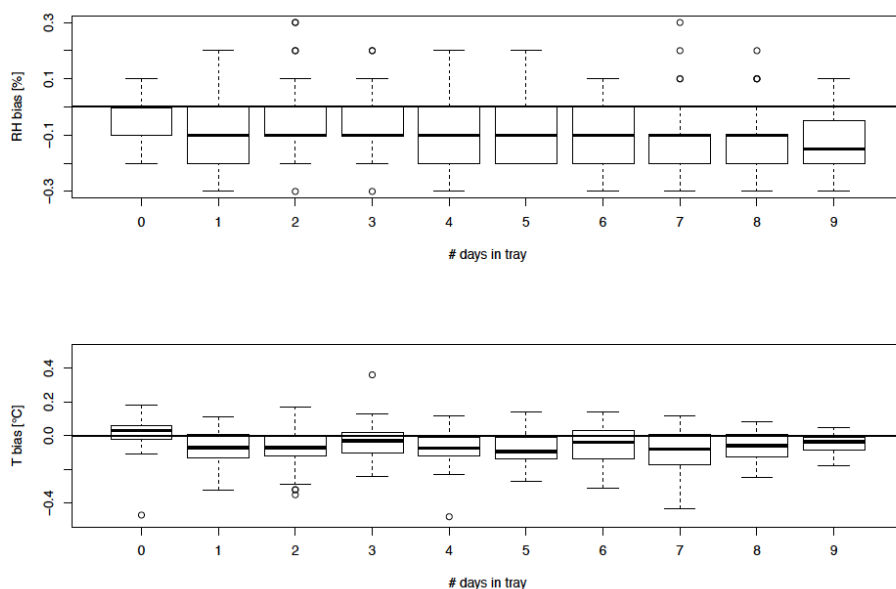
563

564 Figure 9: Mean difference and standard deviation of the RH measured with the manual and automatic system in
 565 Sodankylä at different height interval, from the ground to 15 km a.g.l., as a function of the time period between GC and
 566 launch; from left to the right, the time period increases from 1 to more than 5 days. In brackets within the legend, the
 567 number of parallel soundings considered for each time period is reported.
 568

569 In Figure 10, another way to study GC data is presented for the Payerne station. In this case, the
 570 average difference and the standard deviation of temperature and relative humidity found during
 571 the GC using Vaisala RS41 radiosondes into the Vaisala AS15 versus the aging (up to 9 days into tray
 572 from the loading until launch) is shown. For both temperature and relative humidity, excluding only
 573 the launches which occurred within 24 hours of the radiosonde loading, the bias is negative and
 574 independent of any further aging. Until one day after loading the bias is stable close to zero and
 575 thereafter it increases to about -0.1 K and -0.1% over the following days. These results show how
 576 the use of ARLs also in remote places or where it is required to upload in advance a large number
 577 of radiosondes, to launch with a few days of delay, do not appreciably lead to changes in the Vaisala
 578 GC.

579

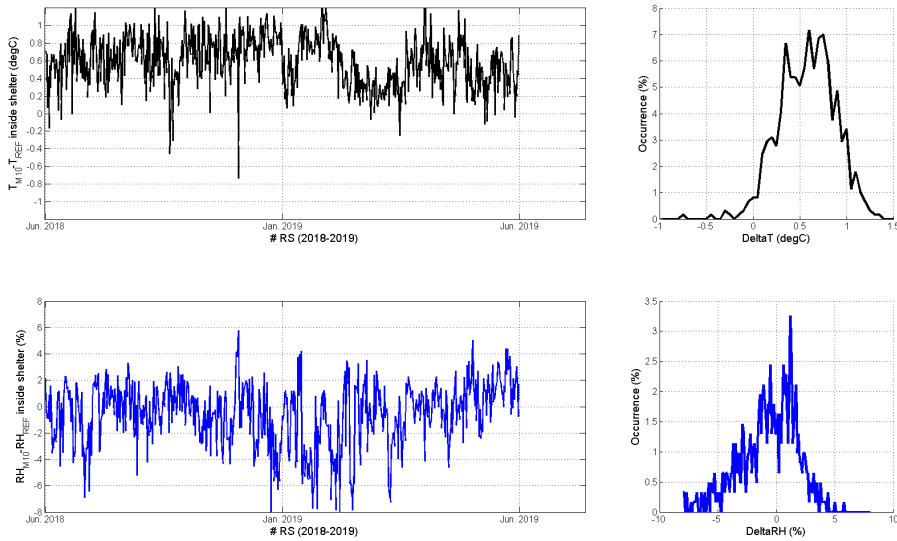
Commentato [FM1]: According to the reviewer #2, these lines were repeated, not this is not the case anymore. The mistaken duplication of the text was removed.



580
 581 Figure 10: Average difference and standard deviation of temperature and relative humidity found during the Vaisala GC
 582 process versus the aging (number of days into tray from the loading until launch) of the radiosonde RS41 into the
 583 Payerne ARL (Vaisala AS15).
 584

585 **4.2. Performance of the Meteomodem ARL**

586 The performance of the Meteomodem ARL ground-check has been evaluated through the analysis
 587 of a dataset collected at MétéoFrance Trappes station, where M10 radiosondes have been launched
 588 regularly at 11:30 and 23:30 UTC since 2016. The availability of a long time series for the comparison
 589 between M10 temperature and humidity sensor and a reference temperature/humidity sensor
 590 (Vaisala HMP110, [https://www.vaisala.com/sites/default/files/documents/HMP110-Datasheet-](https://www.vaisala.com/sites/default/files/documents/HMP110-Datasheet-B210852EN_1.pdf)
 591 [B210852EN_1.pdf](https://www.vaisala.com/sites/default/files/documents/HMP110-Datasheet-B210852EN_1.pdf)) at ambient conditions, inside a meteorological shelter for the Trappes station,
 592 permits the investigation of the system performance also in the pre-launch phase. Since June 2018,
 593 this comparison is carried out during the 5 minutes before each automatic sounding. Figure 11
 594 summarizes the time series and PDF of the difference between M10 and HMP110 sensor for
 595 temperature (black curve, upper panel) and relative humidity (blue curve, lower panel) recorded
 596 between June 2018 and June 2019. The relative humidity difference oscillates around 0% and in
 597 more than 75% of the cases the difference is smaller than 2% RH in absolute value. For temperature,
 598 the observed residual difference around 0.5°C requires further investigations.
 599



600
 601 Figure 11: Time series and pdf of the difference between M10 and HMP110 sensor for temperature (black curve) and
 602 relative humidity (blue curve) between June 2018 and June 2019, measured at ground level inside a meteorological
 603 shelter in ambient condition.

604
 605 Figure 12 provides a picture of the meteorological shelter and the position of the HMP110 and the
 606 M10 during the 5-minutes comparison shown in Figure 11. These results need further investigations
 607 in order to determine if the systematic difference observed on temperature in the meteorological
 608 shelter is due to the Meteomodem M10 batches produced in 2018, though Meteomodem did not
 609 report similar systematic differences during the production checks, or if this could be due to the
 610 need for improvements in the experimental protocol. The meteorological shelter has been
 611 improved with the installation of a fan (Figure 12) which should produce a better homogenisation
 612 of the temperature and relative humidity around the two sensors. The development of a new
 613 experimental protocol is under consideration and should lead to the production of a tube ventilated
 614 by a laminar flow in which the Meteomodem M10 and a PTU reference could measure under the
 615 same environment, elucidating further upon the characterization of the spatial homogeneity of the
 616 temperature and relative humidity.

617



618

619 Figure 12: Picture of the meteorological shelter in Trappes (left panel: general view: the meteorological is near the
620 Meteomodem ARL entrance for simplicity reasons, right panel: inside of the meteorological shelter)

621

622 Finally, the M10 radiosonde is put inside a SHC chamber for 3 minutes before the sounding (with a
623 relative humidity near 100%): more than 95% of the samplings are accepted after the test. For
624 operational reasons, the Meteomodem probes used in the GRUAN protocol are tested in the
625 meteorological shelter and in the 100% RH test but not necessarily in this order each time. It is not
626 known if the order of the checks makes any difference.

627

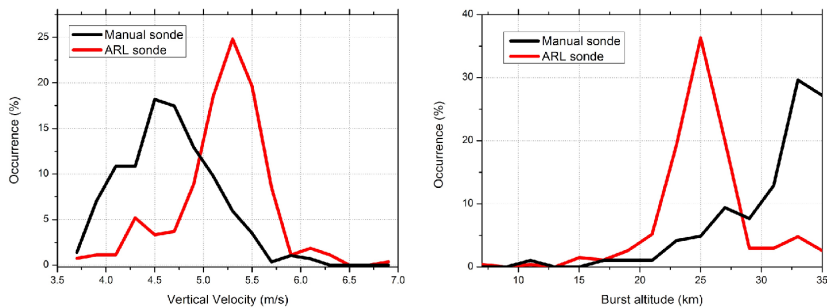
628 5. Vertical velocity and balloon burst

629 This section reports the statistics for the vertical velocity and the balloon burst altitudes from the
630 datasets collected at Sodankylä and Trappes stations.

631 5.1 Vertical velocity and balloon burst altitude for Vaisala technology

632 In Figure 13, the statistics of the balloon vertical velocity and of the burst altitude for Sodankylä in
633 the period from 2006 to 2012 are shown. In terms of vertical velocity (Figure 13, left panel), the ARL
634 has a quasi-symmetric frequency distribution peaked around 5.3 m s^{-1} with a spread mainly between
635 4.7 m s^{-1} and 5.9 m s^{-1} . For the manual launches, the frequency distribution is quite wide, non-
636 symmetric, peaked around 4.5 m s^{-1} with a larger spread of the values mainly between 3.5 m s^{-1} and
637 5.7 m s^{-1} . The comparison reveals the higher stability of the ARL compared to manual launches in

638 controlling the balloon filling and, therefore, the sounding vertical velocity which is relevant for the
 639 quality of the measured profile. For the balloon burst altitude (Figure 13, right panel), a like-for-like
 640 comparison between the manual launches and the ARL is not feasible at Sodankylä due to the use
 641 of different balloon types (typically smaller for the ARL) which causes a strong difference in balloon
 642 altitude. Totex Tx800 or Tx600 type of balloons were used in winter and Totex Ta350 or Tx350 type
 643 sounding balloons were flown during all other seasons. Due to smaller balloon volume, the
 644 summertime soundings had lower burst heights on average. The burst altitude for the ARL has also
 645 in this case a quasi-symmetric frequency distribution peaked around 25 km of altitude a.g.l with a
 646 spread of the values mainly between 17 km and 28 km a.g.l., while the distribution for manual
 647 launches is non-symmetric, with a maximum frequency around 33 km and most of values ranging
 648 within 21 - 35 km a.g.l. Differences between night-time and day-time soundings were not significant,
 649 although night time soundings have on average lower burst heights during polar vortex overhead
 650 conditions in winter.
 651



652
 653

654 Figure 13: Vertical velocity (left panel) for radiosondes launched manually (black line) and automatically (red line), along
 655 with burst altitude (right panel) at Sodankylä station.

656

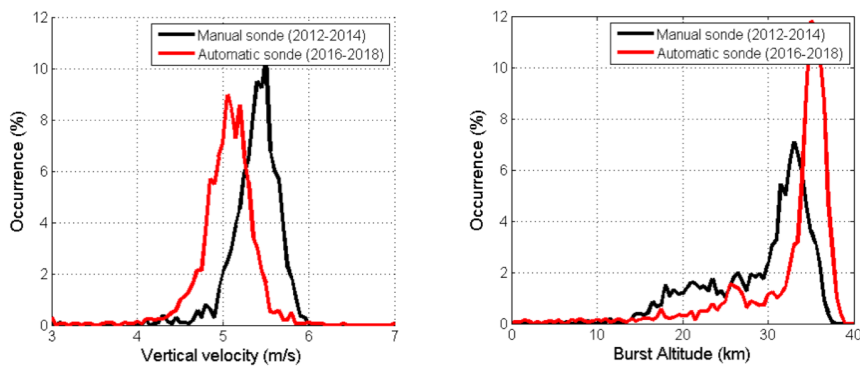
657 **5.2 Vertical velocity and balloon burst altitude for Meteomodem technology**

658 A more interesting comparison to show the eventual positive influence of automation on the burst
 659 altitude is those related to the dataset discussed in Section 3 and summarized in Table 5, shared by
 660 Météo France for Trappes station (Figure 14). In terms of vertical velocity (Figure 14, left panel),
 661 both the ARL and the manual launches have a quasi-symmetric frequency distribution peaked
 662 around 5.1 m s^{-1} and 5.5 m s^{-1} , respectively, with a similar spread of about 1.0 m s^{-1} . For the burst

663 altitude (Figure 14, right panel), we have for both the datasets a negatively skewed distribution with
 664 an evident peak around 33 km for the manual launches and 35 km for the ARL. The comparison
 665 reveals that the burst altitude (Figure 14, right panel) is generally higher for the ARL than for the
 666 manual launches, likely due to use of different balloons and the more limited human contact with
 667 the balloon which hence likely retains greater structural integrity. ARL frequency distribution has
 668 also a more peaked distribution that can be related to a more homogeneous balloon inflation
 669 (automatic inflation, same method, constant gas flow, more stable temperature). Furthermore, the
 670 vertical velocity of the balloon is stable (Figure 14, left panel). 40 % of the balloons burst before 30
 671 km during the manual period, where only 20 % do during the automatic period. This result means
 672 that the Meteomodem ARL and/or the operational procedures, elaborated under a joint effort by
 673 Meteomodem and MeteoFrance, has increased by a factor two the number of balloons reaching an
 674 altitude higher than 30 km. The burst altitude for both periods (2012-2014 for the manual launches
 675 and 2016-2018 for the ARL) shows some seasonal signal. It appears that burst altitude is lower
 676 during the winter. A further study could evaluate burst altitude as a function of air temperature or
 677 potential vorticity in order to study the influence of polar vortex and its potential impact on the
 678 burst altitude.

Eliminato: d

679
680



681
682
683 Figure 14: Vertical velocity (left panel) for radiosondes launched manually (black line) and automatically (red line), along
684 with burst altitude (right panel) at Trappes station.
685
686

687

689 **5.3 Quantifying relative performance**

690 In this section, two datasets are investigated to assess the differences in the vertical profiles of
691 temperature and humidity: the set of RS-92 parallel (automatic and manual) soundings performed
692 with the automatic radiosonde launchers at Sodankylä along with a second set of Meteomodem
693 radiosoundings collected at Faa'a station, French Polynesia. These are near-coincident launches but
694 the instruments are on physically distinct balloons which, as they ascend, likely at somewhat
695 different rates if the balloons are not filled identically, will follow subtly distinct pathways leading
696 to offsets in sampling. In the following analysis, given the latitude ϕ , the longitude λ , the Earth's
697 radius R (mean radius = 6371 km), the distance between two balloons (1 and 2) has been calculated
698 using the 'haversine' formula (Sheppard and Soule, 1922) which provides the great-circle distance
699 between two points (i.e., shortest distance over the earth's surface):

700
$$d = Rc$$

701 where

702
$$c = 2 \operatorname{atan2}(\sqrt{a}, \sqrt{1-a})$$

703
$$a = \sin^2\left(\frac{\Delta\lambda}{2}\right) + \cos(\phi_1) \cos(\phi_2) \sin^2\left(\frac{\Delta\lambda}{2}\right)$$

705

706 The haversine formula remains particularly well-conditioned for numerical computation even at
707 small distances – unlike calculations based on the spherical law of cosines. The function “atan2” is
708 described in Glisson (2011).

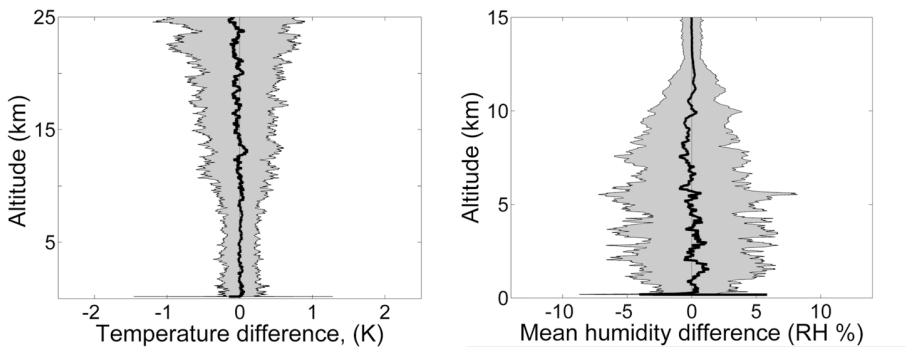
709 The two datasets are also investigated to show the correlation between the difference in the vertical
710 profiles and the distance between the two flying sondes.

711

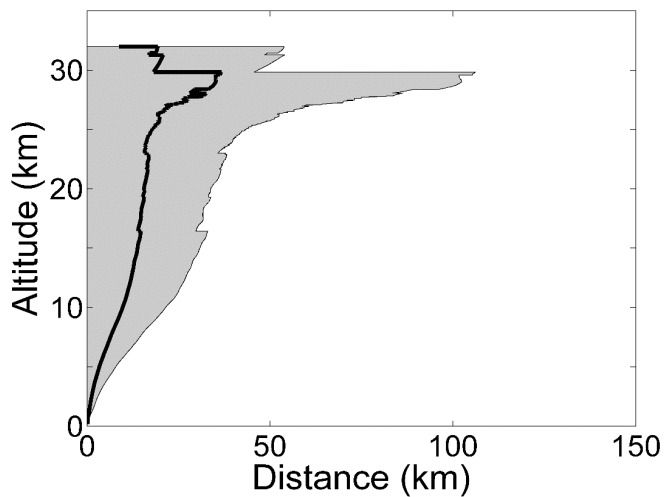
712 **5.4 Parallel soundings with Vaisala systems**

713 For the same six-year dataset collected at Sodankylä discussed in Section 4, the vertical profiles of
714 the average differences (automatic minus manual) and standard deviations of the temperature and
715 RH measured during parallel soundings are shown in Figure 15. Systematic differences in the
716 temperature profile are negligible (on average smaller than 0.01 K) over the entire vertical range up
717 to 25 km a.g.l, while the standard deviation increases with altitude from values smaller than ± 0.5 K
718 below 15 km to values larger than 1 K above. The result is in agreement with the increase in mean
719 distance between near simultaneous sonde paths at higher altitudes (Figure 16). A subset of the
720 parallel temperature soundings at Sodankylä has previously been analyzed by Sofieva et al. (2008).
721 Even though it is hard to separate difference components from non-collocation from those which

722 may arise from instrument-to-instrument differences (e.g. arising from manufacture variations and
723 differences in preparation, storage and launch at the uppermost altitudes), Sofieva et al. found
724 differences in small scale structures in temperature profiles, when the horizontal separation was
725 larger than 20 km. Moreover, to investigate whether the ARL and the manual radiosoundings
726 datasets were selected from populations having the same distribution, i.e. if the calculated mean
727 differences are statistically significant, the Wilcoxon Rank Sum test has been applied. The test result
728 confirms that the two datasets are samples of the same population showing a probability larger
729 than 0.5 for temperature at all the altitude levels below 20 km and larger than 0.1 above, while for
730 RH values the probability is larger than 0.3 over the entire range from the surface to 15 km a.g.l.



731
732 Figure 15: Temperature (left panel) and RH (right panel) mean difference between ARL and manual for the six-year
733 dataset of parallel soundings collected at Sodankylä station at all altitude levels up to 25 km a.g.l for temperature and
734 up to 15 km a.g.l for RH. Standard deviation at each pressure level is reported using the gray area.
735



736

737 Figure 16: Horizontal distance between the balloons calculated for the six-year dataset of parallel soundings collected
 738 at Sodankylä station for all the altitude levels up to 32 km a.g.l.

739

740 For the RH mean difference profile (Figure 15, right panel), there are no significant systematic
 741 differences up to 7 km and then again above 10 km a.g.l., while in between these altitudes a small
 742 negative mean difference lower than 1% RH is found and may be related to the RH variability in the
 743 upper troposphere and the increased distance between the two sondes. The increase in standard
 744 deviation in the lower troposphere below 5 km a.g.l., with values generally smaller than 5% RH, is
 745 due to the high RH variability which can be significant even for small horizontal distances between
 746 the two sondes. Above 5 km, and continuing through the profile to the UT/LS where the values of
 747 RH are on average smaller and less variable, RH difference decreases except when clouds or other
 748 uncommon events are detected (e.g. Stratospheric-Tropospheric exchanges).

749 In addition, the analysis was rerun after grouping the ARL flights according to the time a sonde had
 750 been loaded to the launcher system (see section 4): variations of time period between sonde loading
 751 and actual launch time did not influence the comparison results.

752 Finally, the Wilcoxon Rank Sum Test has been applied to the entire dataset and the computed
 753 probability that the two samples belong to the same population is larger than 0.35 at all altitude
 754 levels.

755

756 **5.5 Parallel soundings at Faa'a with Meteomodem systems**

757 A first evaluation of the performance of Meteomodem ARL is provided by the analysis of the
758 datasets collected over 3-14 October 2018 at Faa'a station (French Polynesia, station identifier=0-
759 20000-0-91938, 17.63S, 149.84W, 21 m a.s.l.) where 21 launches (9 day-time and 12 night-time) of
760 parallel radiosoundings have been undertaken (a picture is provided in Figure 17) in order both to
761 compare temperature, relative humidity, wind speed and direction, and to study further
762 characteristics of the flights (burst altitude, ascent speed for example). Meteo-France has
763 conducted the Intensive Operational Period while Institut Pierre Simon Laplace (IPSL) has produced
764 the NetCDF files (data and metadata) for the analysis. Raw data without any correction for
765 temperature and relative humidity have been considered in this paper. The GRUAN data processing,
766 which remains under development at the present time for this datastream, has not been applied.
767 The manufacturer Meteomodem IR2010 software was used for both manual and automatic
768 launches.

769



770

771 Figure 17: Daytime parallel sounding at Faa'a station (French Polynesia).

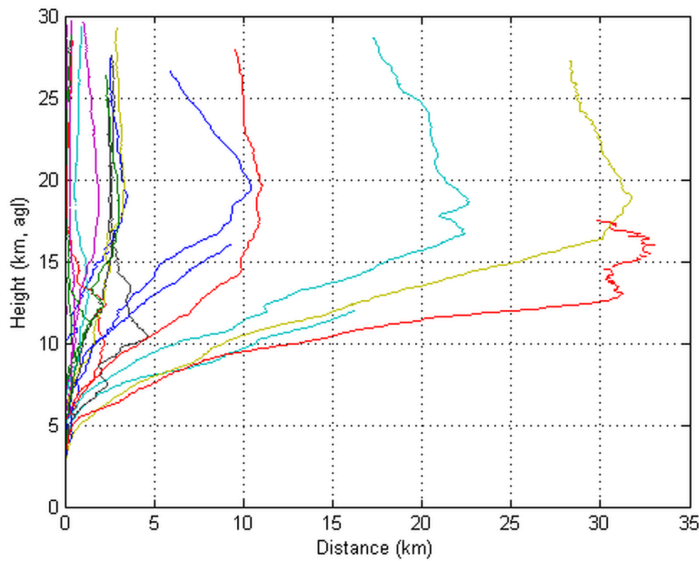
772

773 The dataset collected by Meteo-France at Faa'a station is not sufficiently large to draw robust
774 statistical inferences. Nevertheless, this dataset is the first ever available to evaluate the
775 performances of the Meteomodem ARL and can provide useful indications of any likely impact upon
776 the data quality of ARL facilities.

777 Before comparing, the T and RH profiles of the parallel sounding dataset have been interpolated to
778 a resolution of 100 m altitude. The difference between the launch time of the ARL and the manual
779 balloons ranges between 1 and 12 seconds.

780 In Figure 18, the horizontal distance between the pairs of parallel soundings at all the altitude levels
781 up to 25 km a.g.l is shown: the horizontal distance between the two balloons is typically within
782 about 35 km.

783 In Figure 19, the mean difference between the set of ARL and manual parallel soundings profiles of
784 temperature and RH as a function of altitude regardless of time mismatch, along with the
785 corresponding standard deviation is shown. The left panel of Figure 19 shows the difference for
786 temperature, while the right panel shows it for RH. The mean temperature difference is smaller
787 than ± 0.2 K up to 12-13 km a.g.l., and typically smaller than ± 0.5 K above. The difference is negative,
788 up to -2.0 K, in the first 50-100 meters and this is probably due to the potential warming effect of
789 the ARL environment on the radiosonde sensor.

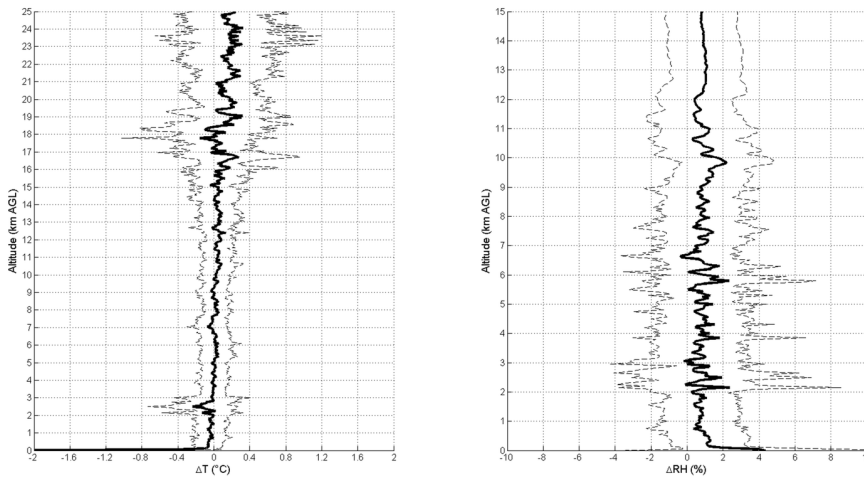


790
791 Figure 18: Horizontal distance calculated for the balloons of the 21 parallel soundings performed at Faa'a station for all
792 the altitude levels up to 25 km a.g.l. Measurement time between the two sondes at the same altitude levels may differ
793 and at the start time ranges within 1-12 seconds.
794

795 For RH, the mean difference is instead always positive and smaller than 0.7% RH up to 8 km a.g.l.
796 with a standard deviation smaller than 3-4% RH. Above 8 km, the mean difference becomes larger
797 and less variable with a maximum of about 2% RH and a standard deviation around 3%. The
798 Wilcoxon Rank rank sum test has been applied to both temperature and RH. For temperature, the
799 probability is higher than 0.3 until 17 km and higher than 0.2 above, while for RH is larger than 0.2

800 below 10 km and larger than 0.1 above. Only in the first 40 m for temperature and the first 20 m for
 801 RH, the Wilcoxon Rank sum test fails with a probability lower than 0.05. The results of the test
 802 confirm the null hypothesis of the same median for the ARL and manual data distribution at all the
 803 height levels for both temperature and RH, with the only exception of a few decameter above the
 804 ground because of the ARL air conditioned effect. The reason behind this bias could arise from GC
 805 effects or differences in the pre-launch procedures between the two systems affecting the
 806 performance of one of the two launches in a quasi-systematic manner throughout the vertical
 807 profile. This will be further investigated with the support of the manufacturer.

808 In terms of balloon burst altitude the ARL proved to be reliable both during the daytime with a burst
 809 altitude ranging within 26688 - 31904 m above ground level (a.g.l.) versus values within 24970 -
 810 30621 m a.g.l. calculated for the manual launches, while during nighttime the burst altitude ranges
 811 within 27587 - 30790 m a.g.l. for the automatic launcher versus values within 27437 - 30139 m a.g.l.
 812 for the manual launches. Applying the Wilcoxon Rank-Sum Test, the computed probability (0.05224)
 813 for the entire dataset is slightly greater than the 0.05 significance level and, therefore, the two
 814 distributions of burst altitudes are not significantly different indicating that ARL does not lead to
 815 significant improvements in the balloon burst altitude.



816
 817 Figure 19: Difference between ARL and manual profiles of temperature (left panel) and RH (right panel) for 21 parallel
 818 soundings performed at Faa'a station up to 25 km a.g.l. for temperature and up to 15 km a.g.l. for relative humidity.
 819 Black lines: mean differences, dashed lines: standard deviation. A negative difference up to -2.0 K for temperature and
 820 smaller than smaller than 3-4% RH is observed in the first 50-100 meters probably due to the potential warming effect
 821 of the ARL environment on the radiosonde sensor.
 822

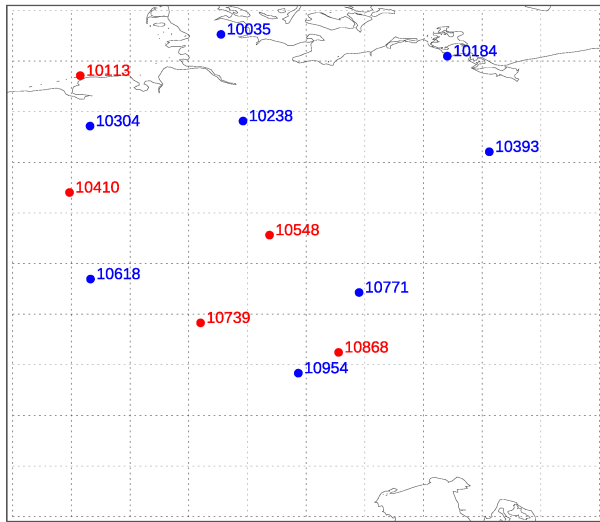
823 **6. Automatic launchers performance evaluated using the ECMWF forecast model**

824 Data assimilation systems compare observations with a short-range forecast (called the
825 background) and use observation-minus-background (O-B) differences in the assimilation to provide
826 improved initial conditions for the next forecast. For some areas/variables the uncertainties in the
827 background are now similar to, or smaller than, those in the observations, so the background
828 provides a very useful comparator. O-B differences from reanalyses have been also used to
829 homogenise historical radiosonde data (Haimberger et al., 2012). Ingleby (2017) compared different
830 radiosonde types with ECMWF background fields and for temperature and upper-tropospheric
831 humidity found differences in radiosonde performance that are broadly consistent with the results
832 of the last WMO radiosonde intercomparison (Nash et al., 2011) and are dominated by the sonde
833 type.

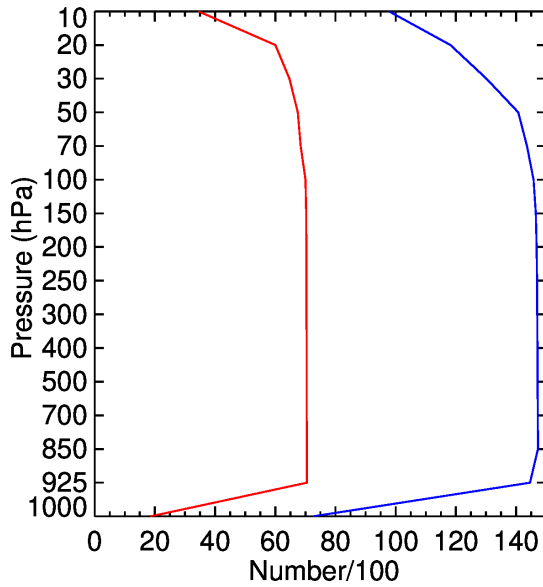
834 Statistics for Vaisala and Meteomodem radiosondes (manned and ARL) were produced. For Vaisala
835 we examined the German radiosondes (Figure 20) which form a relatively dense, well maintained
836 network with manned and ARL stations interspersed - ideal for this type of comparison. The
837 background uncertainties vary somewhat over time and regionally - they are probably slightly larger
838 over the UK because of the proximity of the North Atlantic. The Meteomodem samples were quite
839 small (from five French stations in total) and inconclusive; therefore, they will not be shown. No
840 attempts to provide a comparison of O-B statistics for Meisei ARL stations were carried out. This is
841 due to the fact that all four Meisei ARLs are on small islands, three to the south of the main islands
842 of Japan and one to the south-east, whereas the manned stations are on the main islands (or two
843 distant islands). Therefore, the O-B comparison could be affected by differences in the
844 background uncertainties over the southern islands relative to the main islands.

845 Figure 21 shows the numbers of reports at standard levels for German RS92 launches in the period
846 2017-2019 June. There are more than twice as many manned launches as ARL ascents because four
847 of the manned stations usually report four times per day whereas the other four manned stations
848 and the five ARL stations report twice a day. One interesting feature is that the proportion of ARL
849 ascents reaching 20 hPa is significantly higher than the proportion of manned ascents. A plausible
850 explanation for this is that ARLs put less stress on the neck of the balloon than manual launches
851 (Tim Oakley, pers. comm. 2018). During the middle months of 2017, there was a transition from
852 Vaisala RS92 to Vaisala RS41 at German stations - the proportions of RS41 reports at different
853 standard levels (not shown) are very similar to those in Figure 20.

854



855
 856 Figure 20: The main German radiosonde sites (two training/test sites not shown) and station identifiers: blue - manned
 857 stations (8), red - autosondes (5), as in early 2019 and for several years before that.
 858

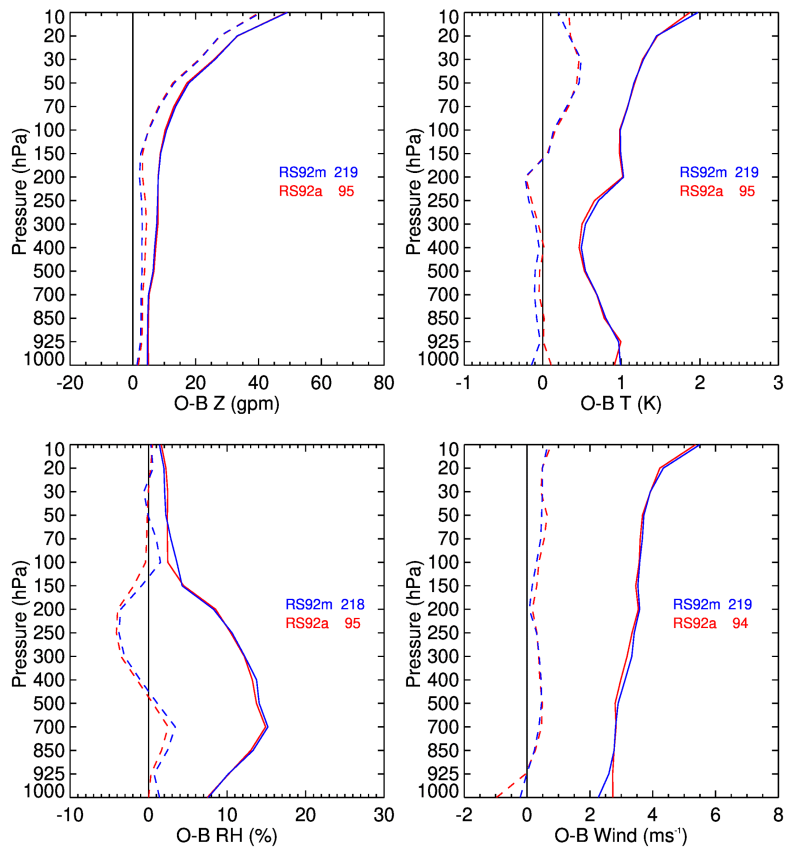


859
 860 Figure 21. The number of temperature reports (hundreds) at standard levels, hPa, from German stations using Vaisala
 861 RS92 radiosondes, 2017-2019 June: blue - manned stations, red - autosondes. The numbers for other variables are very
 862 similar. There are fewer reports at 1000 hPa, and to some extent at 925 hPa, because these levels can be below the
 863 launch site. The decrease at upper levels is due to balloon burst.

864

865 Figures 22 and 23 compare O-B mean and root-mean-square (rms) statistics for German RS92 and
866 RS41 reports respectively (for technical reasons alphanumeric TEMP reports were used rather than
867 binary BUFR reports, see Ingleby and Edwards, 2014). The RS92 results (Figure 22) are very similar
868 between manned and ARL stations (small differences at 1000 hPa are presumably due to the
869 proximity of the surface and relatively small samples). The upper tropospheric humidity has minor
870 systematic differences probably due to humidity time-lag and radiation corrections being
871 introduced at different dates at different stations.

872



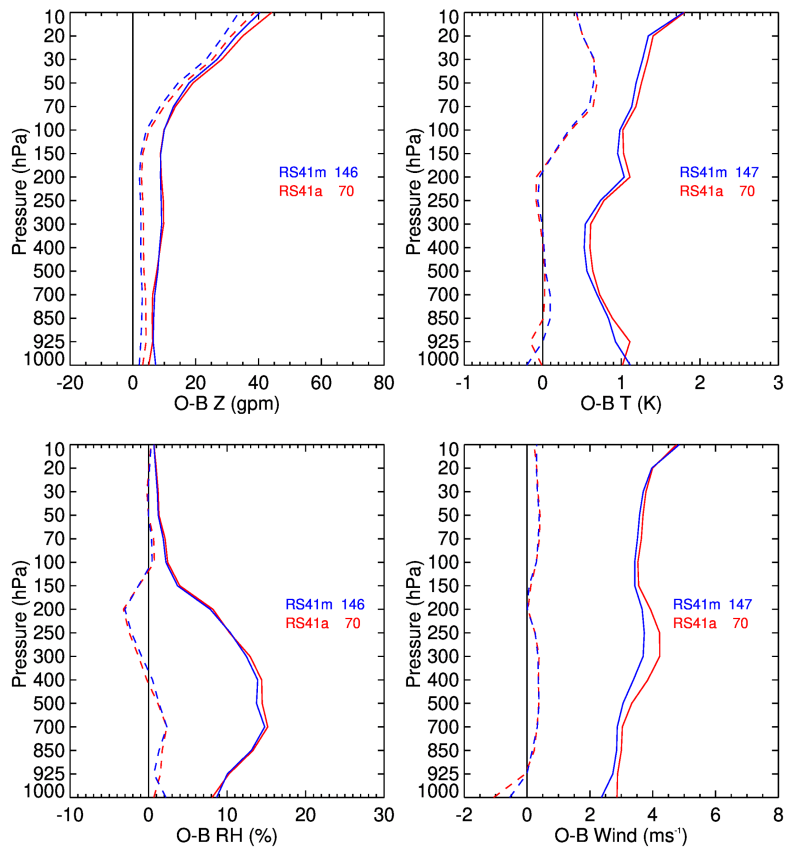
873

874 Figure 22: Mean (dashed) and rms (solid) O-B statistics for German RS92 ascents, 2015-2017: blue - manned, red - ARL.
875 Results for geopotential height (top left), temperature (top right), relative humidity (bottom left) and wind (mean wind
876 speed and rms vector wind; bottom right). The key gives the radiosonde code (RS92m for manual or RS92a for ARL) and
877 the number of reports in hundreds.

878

879 In contrast and surprisingly, the RS41 results (Figure 23) show rather larger rms(O-B) differences for
880 ARL stations - especially for temperature and wind. Qualitatively similar results for RS41 are found
881 for subsets of the period considered confirming the robustness of the results. The reasons for the
882 larger ARL rms differences in Figure 23 are not clear yet; one possibility is linked to the accuracy of
883 the reported pressure values. Pressure is measured by the RS92. For the RS41-SG the pressure is
884 calculated starting from a surface pressure measurement, but the German stations use the RS41-
885 SGP with a pressure sensor. Discussions with Vaisala and DWD (the German weather service) have
886 not so far revealed the cause.

887



888

889 Figure 23: As Figure 22 but for RS41 reports, 2017-June 2019. For some months, all stations reported as type 23 (123
890 in BUFR) so they had to be separated using the station identifiers.

891

892

893

7. Summary and discussion

894

895

896

897

898

899

900

901

902

903

904

905

906

907

908

909

910

911

912

913

914

915

916

917

918

919

920

921

922

In this paper, the existing Automatic Radiosonde Launchers available on the market (Vaisala, Meteomodem and Meisei) are presented and a first comparative analysis of the performance, relative to the more prevalent practice of manual launches, for the two most mature systems at present (Vaisala and Meteomodem) has been reported. The analysis is limited to the data available from a few GRUAN certified or candidate sites (Sodankylä, Payerne, Trappes, Potenza, Faa'a) and to the investigation of the O-B bias and rms using the ECMWF forecast model and the Vaisala ARLs and manual stations of the DWD. The data analysis allows us to infer the following principal conclusions:

- From a technical point of view, the performance of ARL is fully similar or superior to that achieved with the traditional manual launches due to the capability of the automatic launchers to fully control several parameters during the different phases of the radiosonde preparation and balloon launch. This reduces launch-to-launch variability typical in manual launches.
- Despite having some potential advantages, there are still some issues generating failure in the launches which can be improved according to the feedback provided by the GRUAN sites, operating mainly Vaisala ARLs, such as the not infrequent failure of the power supply system or of the air conditioning system, plenty of issues related to the balloon release in the vessel area, likely contributing to early balloon bursts, and to the management of the gas flow to fill the balloon, while the ready-to-launch sondes storage area appears to be the most efficient part of ARLs.
- For both temperature and relative humidity, the GC correction has been investigated for the Vaisala ARL, finding a negative offset relative to manual launch procedures at different stations and considering different radiosonde types (RS92/RS41) and batches of a few tenths of degree and % RH, respectively. For the Meteomodem ARL at Trappes station, the difference between M10 temperature and humidity sensor and the Vaisala HMP110 housed in the ARL, used as a reference immediately prior to launch shows a few tenths of degree and % RH, respectively. These results need further investigation to understand the underlying reasons and whether manual or ARL operations are closer to the observed atmospheric profiles.

Eliminato: Sondakyla

924 ● Systematic differences in the temperature profile for both Meteomodem and Vaisala are
925 smaller than ± 0.2 K up to 10 hPa; RH profile differences are smaller than 1% RH for the
926 Sodankylä Vaisala dataset up to 300 hPa, while it is constantly positive and smaller than 2%
927 for Faa'a station Meteomodem series. However, the restricted dataset available at Faa'a
928 station means caution should be applied in generalizing these results as representative of
929 all Meteomodem ARL.

930 ● O-B mean and rms statistics for German RS92 and RS41 are very similar between manned
931 and ARL stations. The upper tropospheric humidity has minor systematic differences
932 probably due to humidity time-lag and radiation corrections being introduced at different
933 dates at different stations. The RS41 sondes shows larger rms(O-B) differences for ARL
934 stations than RS92, in particular for temperature and wind. The accuracy of the reported
935 pressure values might be a possible reason to explain this difference.

936

937 As mentioned at the beginning of section 3, the factor limiting adoption of ARL radiosounding
938 products within the GRUAN reference network is mainly related to the use of independent and
939 traceable calibration standards like the Standard Humidity Chamber (SHC) within the ARLs. At
940 present, for the different ARLs, this is possible but only before the sonde loading in the ARL trays.
941 GRUAN Data Processing (GDP) is currently applied to the ARL soundings performed by the GRUAN
942 stations though the related measurement programs cannot as yet be certified as GRUAN products.
943 The present analysis has provided a substantive move forwards towards this aim by showing that
944 performance is broadly comparable to manual launches.

945 In the last five years, several discussions within and outside the GRUAN community, involving also
946 the manufactures, allowed to identify a few possibilities to meet the full traceability for the ARLs.
947 Identified solutions to test are related to two main options:

- 948 ● Use of a SHC (plus a reference thermometer, such as PT100 sonde) immediately after the
949 manufacturer GC and prior to loading the sondes;
- 950 ● Use of reference thermometer and hygrometer within the the ready-to-launch sondes
951 storage area, as close as possible to the radiosonde sensors, with the optional use of a few
952 additional thermometers and hygrometers within the storage area to monitor the
953 uniformity of the temperature and relative humidity within the same area.

954 Both approaches have advantages and drawbacks. The first allows use of the SHC as a traceable
955 calibration standard at or around 100 % relative humidity, depending on the solution used in the

956 SHC. Nevertheless, the proposed two stage procedure can be applied only in advance of the launch
957 and tests are needed to confirm what was already shown in Section 4 at Sodankylä and Payerne
958 stations, i.e. a sonde can be launched within a few days from its upload in the ARL without differing
959 significantly from the SHC collected data.

960 The second approach can instead continuously monitor the radiosonde during the entire launch
961 procedure in the storage area and before the sonde tray is moved out to the vessel area for launch,
962 when temperature and RH within the storage area may rapidly change because of the incoming air
963 from outside the vessel area. This approach cannot directly use traceable calibration standards but
964 it must be based on the comparison with reference thermometers and hygrometers calibrated on
965 a routine and certified basis. In addition, the sonde calibration cannot be monitored at 100 % RH
966 because the air conditioning system within the ARL keeps stable humidity conditions and cannot be
967 modified to avoid an impact on the ARL operation efficiency.

968 For both the approaches above, a customized solution to collect the data and use them in the
969 generation of a GDP must be found given the constraints of the ARL software which does not allow
970 extra calibration or comparison values to be collected or saved in the main radiosonde launch files.

971 It must be noted that at 4 JMA stations, not belonging to GRUAN, the Vaisala ARL is used adopting
972 a modified setup of the AS15 system including an additional GC based on reference instruments
973 developed by Vaisala for temperature and humidity, i.e Vaisala HMP155 with HMT333, lodged in a
974 custom-made chamber. When loading the radiosonde, the JMA specified GC for temperature and
975 humidity is also performed, in line with JMA's rule for upper air observations, specifying that the
976 PTU radiosonde sensors should be compared to reference sensors before launch only to confirm
977 that the difference is within a pre-defined threshold, while reference values are not used for any
978 correction of the measured profiles. The JMA additional GC is not a traceable calibration standard
979 and does not allow to perform the 0% RH and 100% RH ground calibration immediately before the
980 launch. Instead, it can be made when the radiosonde is uploaded in the ARL using a method to save
981 the measured comparison values.

982 More details on the JMA specified ground check for temperature and humidity are available at:
983 <https://www.vaisala.com/sites/default/files/documents/RI41-Datasheet-B211322EN.pdf>.

984 The compilation of the table of ARL systems in Appendix A (also the plot in Figure 1) brought home
985 that it is not easy for users to know which stations are using ARLs. We recommend that information
986 on automated launchers (type, start date, end date if appropriate) should be included in the
987 OSCAR/Surface catalogue.

988 Other issues which must be considered and solved to provide a GDP from ARLs are related to the
989 need to supply the manufacturer software with an accurate local pressure measurement and its
990 height at the launch time. Delays between the actual and the reported launch time from the
991 software is another issue which is under investigation by the GRUAN community.

992 The GRUAN community is discussing a strategy to achieve the full traceability for the ARL products
993 and to ascertain if any of the approaches described above can be tested intensively at one or more
994 sites: unfortunately, many of the GRUAN sites are also operational stations from the Met Services
995 and from other research institutions and are not readily available for testing. The next step will be
996 to identify which sites can perform specific tests on the ARL traceability and to collect as many
997 metadata as possible from all the GRUAN sites to report, in following publications, extensive
998 statistics validating the results presented in this paper.

999

1000 **8. Author contribution**

1001 Fabio Madonna with the help of Rigel Kivi and Masatomo Fujiwara worked on the paper
1002 conceptualization and on the methodology. Fabio Madonna, Rigel Kivi, Jean-Charles Dupont, Bruce
1003 Ingleby, Gonzague Romanens, Miguel Hernandez, Masami Iwabuchi, Shunsuke Hoshino and Peter
1004 Thorne have been involved in the formal analysis. All the co-authors contributed to the writing of
1005 original draft, review and editing.

1006

1007 **9. Competing interests**

1008 The authors declare that they have no conflict of interest.

1009

1010 **10. Acknowledgements**

1011 Much useful information has been provided by the three manufacturers: Vaisala, Meteomodem and
1012 Meisei. Information on which stations use Meteomodem ARLs was provided by Adrien Ferreira of
1013 Meteomodem in April 2019. Hannu Jauhiainen of Vaisala provided a list of stations using their
1014 Autosonde including several which were not known from the WIS reports. MeteoFrance and several
1015 other National Meteorological Services have also provided information. The Faa'a data discussed in
1016 this manuscript are available at ftp://ftp.lmd.polytechnique.fr/jcdupont/data_m10_gruan_faa and
1017 can be used or cited under the DOI number <https://doi.org/10.14768/20181213001.1>.

1018

1019 **11. References**

1020 Bodeker, G. E., Bojinski, S., Cimini, D., Dirksen, R., Haeffelin, M., Hannigan, J. W., Hurst, D. F., Leblanc,
1021 T., Madonna, F., Maturilli, M., Mikalsen, A., Philipona, R., Reale, T., Seidel, D., Tan, D., Thorne, P.,
1022 Vömel, H. and Wang, J.: Reference upper-air observations for climate: From concept to reality,
1023 Bulletin of the American Meteorological Society, 97 (1), pp. 123-135. doi: 10.1175/BAMS-D-14-
1024 00072.1, 2016.

1025

1026 Carminati, F., Migliorini, S., Ingleby, B., Bell, W., Lawrence, H., Newman, S., Hocking, J., and Smith,
1027 A.: Using reference radiosondes to characterise NWP model uncertainty for improved satellite
1028 calibration and validation, Atmos. Meas. Tech., 12, 83–106, [https://doi.org/10.5194/amt-12-83-](https://doi.org/10.5194/amt-12-83-2019)
1029 2019, 2019.

1030

1031 Dirksen, R. J., Sommer, M., Immler, F. J., Hurst, D. F., Kivi, R., and Vömel, H.: Reference quality upper-
1032 air measurements: GRUAN data processing for the Vaisala RS92 radiosonde, Atmos. Meas. Tech., 7,
1033 4463-4490, <https://doi.org/10.5194/amt-7-4463-2014>, 2014.

1034

1035 Glisson, T. H.: Introduction to Circuit Analysis and Design, Springer Science & Business Media, Ed. 1,
1036 XV, 768, 10.1007/978-90-481-9443-8, 2011.

1037

1038 Haimberger, L., C. Tavolato, S. Sperka: Homogenization of the Global Radiosonde Temperature
1039 Dataset through Combined Comparison with Reanalysis Background Series and Neighboring
1040 Stations, J. Clim., 25, 8108–8131, doi:10.1175/JCLI-D-11-00668.1, 2012.

1041

1042 Ho, S.-P., Peng, L., and Vömel, H.: Characterization of the long-term radiosonde temperature biases
1043 in the upper troposphere and lower stratosphere using COSMIC and Metop-A/GRAS data from 2006
1044 to 2014, Atmos. Chem. Phys., 17, 4493-4511, <https://doi.org/10.5194/acp-17-4493-2017>, 2017.

1045

1046 Ingleby B, Edwards D.: Changes to radiosonde reports and their processing for numerical weather
1047 prediction, Atmosph. Sci. Lett., 16: 44-49. doi: 10.1002/asl2.518, 2014

1048

1049 Ingleby, B.: An assessment of different radiosonde types 2015/2016. ECMWF Tech. Memo. 807, 69
1050 pp., [https://www.ecmwf.int/sites/default/files/elibrary/2017/17551-assessment-different-](https://www.ecmwf.int/sites/default/files/elibrary/2017/17551-assessment-different-radiosonde-types-20152016.pdf)
1051 [radiosonde-types-20152016.pdf](https://www.ecmwf.int/sites/default/files/elibrary/2017/17551-assessment-different-radiosonde-types-20152016.pdf), 2017.

1052

1053 Kobayashi, E., Hoshino, S., Iwabuchi, M., Sugidachi, T., Shimizu, K., and Fujiwara, M.: Comparison of
1054 the GRUAN data products for Meisei RS-11G and Vaisala RS92-SGP radiosondes at Tateno (36.06° N,
1055 140.13° E), Japan, Atmos. Meas. Tech., 12, 3039–3065, <https://doi.org/10.5194/amt-12-3039-2019>,
1056 2019.

1057

1058 Kostamo, P., Advanced automation for upper-air stations, WMO Instruments and Observing
1059 Methods Report No. 49 (TECO-92), pp. 104-107.
1060 https://library.wmo.int/index.php?lvl=notice_display&id=11254#Xeo3GS2h01l, 1992

1061

1062 Lehtinen, R., T. Tikkanen, J. Räsänen, and M. Turunen: Factors contributing to RS41 GPS-based
1063 pressure and comparison with RS92 sensor-based pressure, WMO Technical Conference (TECO), St.
1064 Petersburg, Russia. [https://www.wmo.int/pages/prog/www/IMOP/publications/IOM-116_TECO-](https://www.wmo.int/pages/prog/www/IMOP/publications/IOM-116_TECO-2014/Session%201/P1_28_Lehtinen_RS41PressCompRS92.pdf)
1065 [2014/Session%201/P1_28_Lehtinen_RS41PressCompRS92.pdf](https://www.wmo.int/pages/prog/www/IMOP/publications/IOM-116_TECO-2014/Session%201/P1_28_Lehtinen_RS41PressCompRS92.pdf), 2014.

1066

Codice campo modificato

Codice campo modificato

1067 Lilja A., Franssila J., Hautaniemi P., Lehmuskero M. Review of the History and Future of Automatic
1068 Upper Air Soundings. TECO-2018, Amsterdam, the Netherlands. October 8th - 11th, 2018.
1069
1070 Madonna, F., Amodeo, A., Boselli, A., Cornacchia, C., Cuomo, V., D'Amico, G., Giunta, A., Mona, L.,
1071 and Pappalardo, G.: CIAO: the CNR-IMAA advanced observatory for atmospheric research, *Atmos.*
1072 *Meas. Tech.*, 4, 1191-1208, <https://doi.org/10.5194/amt-4-1191-2011>, 2011.
1073
1074 Madonna, F., Rosoldi, M., Güldner, J., Haefele, A., Kivi, R., Cadetdu, M. P., Sisterson, D., and
1075 Pappalardo, G.: Quantifying the value of redundant measurements at GCOS Reference Upper-Air
1076 Network sites, *Atmos. Meas. Tech.*, 7, 3813-3823, <https://doi.org/10.5194/amt-7-3813-2014>, 2014.
1077
1078 Nash J., T. Oakley, H. Vömel, and Wei Li.: WMO Intercomparison of High Quality Radiosonde
1079 Systems Yangjiang, China, 12 July - 3 August 2010, WMO Instruments and Observing Methods
1080 Report No. 107, 2011.
1081
1082 Sheppard, W. W., and C. C. Soule: Practical navigation, World Technical Institute, Jersey City, 1922.
1083
1084 Sherwood, S. C., C. L. Meyer, R. J. Allen, and H. A. Titchner: Robust tropospheric warming revealed
1085 by iterative homogenized radiosonde data, *J. Clim.*, 21, 5336–5352, doi:10.1175/2008JCL2320.1,
1086 2008.
1087
1088 Sofieva, V. F., F. Dalaudier, R. Kivi, and E. Kyrö: On the variability of temperature profiles in the
1089 stratosphere: Implications for validation, *Geophys. Res. Lett.*, 35, L23808,
1090 doi:10.1029/2008GL035539, 2008.
1091
1092 Thorne, P. W., D. E. Parker, S. F. B. Tett, P. D. Jones, M. McCarthy, H. Coleman, and P. Brohan:
1093 Revisiting radiosonde upper-air temperatures from 1958 to 2002. *J. Geophys. Res.*, 110, D18105,
1094 doi:10.1029/2004JD005753, 2005.
1095
1096 Vaisala: Vaisala Radiosonde RS41 Measurement Performance White Paper. Ref. B211356EN-A ©
1097 Vaisala, 2013.
1098
1099 Vaisala: Comparison of Vaisala Radiosondes RS41 and RS92 White Paper. Ref. B211317EN – B ©
1100 Vaisala, Helsinki, Finland, 2014. Vaisala: Vaisala Radiosonde RS41 White Paper – Ground Check
1101 Device R141. Ref. B211539EN-A © Vaisala, 2015.
1102
1103
1104

1105 12. APPENDIX A: Table of ARL systems operating around the world

1106 Table A1: ARL stations shown in Figure 1. For each station, the WMO ID, which is also part of the WIGOS code
1107 (<https://oscar.wmo.int/surface>), the latitude, the longitude, the country and the period of installation is reported. For
1108 the approximate installation date (year or year-month), the metadata have been collected from different sources (IGRA,
1109 ECMWF, manufacturers, personal communication from scientists and instrument operators). If the last column is empty,
1110 no clear information on the installation period at that station are available. For Vaisala systems the "radiosonde type"
1111 in the reports should indicate if an ARL is being used, but it has been found that this is not always coded correctly. For

1112 Modem and Meisei systems there is no way for the current code formats to indicate that an ARL has been used. The
 1113 list is ordered according to the WMO ID.
 1114
 1115

WMO ID	Latitude	Longitude	Country	Installed
01001	70.940	-8.668	Norway	Meteomodem 2019-09
01010	69.315	16.131	Norway	Vaisala 2014
01241	63.705	9.612	Norway	Vaisala 2001
01415	58.874	5.665	Norway	Vaisala 2013
01492	59.943	10.719	Norway	Vaisala 1997
02185	65.543	22.115	Sweden	Vaisala 1996
02365	62.532	17.436	Sweden	Vaisala 1994
02527	57.657	12.291	Sweden	Vaisala 1994
02591	57.671	18.345	Sweden	Vaisala pre-1996
02836	67.366	26.631	Finland	Vaisala 2005-12
02963	60.815	23.499	Finland	Vaisala 1998
03238	55.019	-1.878	UK	Vaisala 1999
03354	53.006	-1.250	UK	Vaisala 1999
03882	50.891	0.317	UK	Vaisala 2001
03918	54.503	-6.343	UK	Vaisala 2002

03953	51.939	-10.241	Ireland	Meteomodem 2015
04018	63.975	-22.588	Iceland	Vaisala 2006
04360	65.611	-37.637	Greenland	Meteomodem 2012
06610	46.813	6.943	Switzerland	Vaisala 2018
07110	48.444	-4.412	France	Meteomodem 2016-04
07145	48.770	2.010	France	Meteomodem 2015-04
07510	44.831	-0.691	France	Meteomodem 2012-06
07645	43.856	4.407	France	Meteomodem 2011-11
07761	41.918	8.792	France	Meteomodem 2014-06
08190	41.384	2.118	Spain	Meteomodem 2012
08221	40.465	-3.589	Spain	Vaisala 2002
08392	39.606	2.707	Spain	Vaisala 2002
08383	37.278	-6.911	Spain	Vaisala 2018
08430	38.002	-1.171	Spain	Meteomodem 2015
10035	54.527	9.550	Germany	Vaisala 2019-10
10113	53.712	7.152	Germany	Vaisala 2011
10410	51.404	6.968	Germany	Vaisala 2012
10548	50.562	10.377	Germany	Vaisala 2011

Eliminato: 20

10739	48.828	9.201	Germany	Vaisala 2012
10868	48.245	11.553	Germany	Vaisala 2013
11010	48.232	14.201	Austria	Vaisala 2016
11120	47.260	11.355	Austria	Vaisala 2015
11240	46.994	15.447	Austria	Vaisala 2015
13388	43.327	21.898	Serbia	Meteomodem 2015
14430	44.101	15.339	Croatia	Vaisala 1999
16113	44.539	7.613	Italy	Vaisala 1999
16144	44.654	11.623	Italy	Vaisala 1998
45004	22.312	114.173	Hong Kong	Vaisala 2003
47155	35.170	128.573	S Korea	Vaisala 2001
47418	42.953	144.438	Japan	Vaisala 2010-03
47600	37.391	136.895	Japan	Vaisala 2010-03
47678	33.122	139.779	Japan	Meisei (Vaisala from 2003-06 to 2010-03)
47741	35.458	133.066	Japan	Vaisala 2010-03
47778	33.45	135.757	Japan	Vaisala 2010-03
47909	28.393	129.552	Japan	Meisei 2007-03

47918	24.337	124.165	Japan	Meisei 2006-03
47945	25.829	131.229	Japan	Meisei (Vaisala from 2005-03 to 2017-03)
60018	28.318	-16.382	Spain	Vaisala 2001
60096	23.705	-15.930	Morocco	Meteomodem 2012
60155	33.559	-7.667	Morocco	Meteomodem 2014
61980	-20.9	55.500	La Reunion	Meteomodem 2018-04
70026	71.287	-156.763	USA, Alaska	Vaisala 2010
70133	66.885	-162.597	USA, Alaska	Vaisala 2019
70200	64.513	-165.443	USA, Alaska	Vaisala 2019
70219	60.780	-161.838	USA, Alaska	Vaisala 2018
70231	62.953	-155.603	USA, Alaska	Vaisala 2018
70261	64.814	-147.859	USA, Alaska	Vaisala 2018
70273	61.175	-149.993	USA, Alaska	Vaisala 2018
70308	57.167	-170.22	USA, Alaska	Vaisala 2018
70326	58.678	-156.647	USA, Alaska	Vaisala 2019

70350	57.750	-152.494	USA, Alaska	Vaisala 2015
70361	59.503	-139.66	USA, Alaska	Vaisala 2018
70398	55.043	-131.571	USA, Alaska	Vaisala 2018
71964	60.733	-135.097	Canada	Vaisala 1997
78897	16.260	-61.510	Gaudeloupe	Meteomodem 2015
81405	4.830	-52.370	French Guyana	Meteomodem 2012-09
89859	-74.624	164.232	Antarctic (S. Korea)	Vaisala 2014
91592	-22.27	166.450	New Caledonia	Meteomodem 2016-06
91938	-17.63	-149.84	Tahiti	Meteomodem 2018-10
94170	-12.678	141.921	Australia	Vaisala 1998
94302	-22.241	114.097	Australia	Vaisala 1997
94312	-20.373	118.632	Australia	Vaisala 1998
94332	-20.679	139.488	Australia	Vaisala 1998
94430	-26.613	118.536	Australia	Vaisala 1998
94510	-26.414	146.257	Australia	Vaisala 1998

94637	-30.784	121.454	Australia	Vaisala 2000
94653	-32.13	133.698	Australia	Vaisala 1999
94659	-31.156	136.805	Australia	Vaisala 2000
94711	-31.484	145.897	Australia	Vaisala 1997
94776	-32.793	151.836	Australia	Vaisala 2002
94821	-37.748	140.775	Australia	Vaisala 2010
94995	-31.542	159.077	Australia	Vaisala 2010
95527	-29.49	149.847	Australia	Vaisala 1999
96996	-12.189	96.834	Australia	Vaisala 1997

1117
1118
1119
1120
1121
1122
1123
1124
1125

Table A2: Additional ARL systems not transmitting data through the WIS in 2019 or used only for tests and short campaign (not shown in Figure 1). The ARL from 08160 was relocated to 08383.

Identifier	Latitude	Longitude	Country	Installed
POT (GRUAN)	40.600	15.725	Italy	Vaisala 2004
08160	41.660	-1.000	Spain	Vaisala 2005 to 2016
72402 (test)	37.930	-75.480	USA	Vaisala 2014 Meteomodem 2017
71461 (test)	55.810	-117.890	Canada	Vaisala 2016 Meteomodem 2017
10141 (test)	53.650	10.117	Germany	Vaisala 2016

1126